

## *Geology of the Beypazarı trona field, Ankara, Turkey*

**Cahit Helvacı\***

*Dokuz Eylül Üniversitesi, Mühendislik Fakültesi, Jeoloji Mühendisliği Bölümü, Tınaztepe Yerleşkesi, 35160 Buca İzmir, Turkey*

### ABSTRACT

The Beypazarı district is a large area of volcano-sedimentary rocks in the interior of central Anatolia, situated ~100 km northwest of Ankara. Trona, lignite, and bituminous shale occur in the lower part, and Na-sulfate and gypsum occur in the upper part of the sedimentary sequence of the Beypazarı Miocene basin.

The Miocene sequence rests on basement rocks along an angular unconformity; the basement rocks comprise metamorphic, ophiolitic, carbonate and clastic rocks ranging in age from Paleozoic to Eocene. The Miocene sequence has been subdivided into seven sedimentary formations, plus the Teke volcanics. In ascending order, these sedimentary rock units are the Çoraklar, Hırka, Akpınar, Çayırhan, Bozbelen, and Kirmir formations, and the Sarıyar Limestone.

The trona deposit located north of Zaviye village is associated with shale in lower part of the Hırka Formation and alternates with bituminous shale and claystones. Based on borehole data, it is estimated that the areal extent of the trona deposit is ~8 km<sup>2</sup>. The trona beds were deposited as two lensoidal bodies within a 70–100 m thick zone in the lower part of the shale unit. A total of 33 trona beds are known: 16 in the lower trona lens and 17 in the upper lens. The total thickness of the lower trona horizon ranges from 40 to 60 m, and the total thickness of the upper trona horizon is ~40 m. The interval between the lower and the upper trona horizons varies from 30 m to 35 m. The central part of the trona deposit is generally thicker than the marginal parts, and the trona beds grade laterally into dolomitic mudstones and claystones toward the edges of the basin. The total thickness of the trona beds in both lenses varies between 21 and 34 m in the central parts, and 2.5 and 12 m in the marginal parts of the ore bodies. The common thickness of the individual trona beds in both trona horizons ranges from 0.4 m to 2 m. The isopach contours of both trona horizons are restricted by the Zaviye fault.

The principal sodium-carbonate minerals are trona and minor nahcolite occurring in the marginal parts of the trona deposits, and trace amounts of pirssonite and thermonatrite occur locally. Trona and dolomite are associated throughout the trona zone. Calcite, zeolites, feldspars, and clays are the most common minerals within the associated rocks of the trona deposit. Trona crystals, generally white and occasionally grayish due to the presence of impurities, formed massively and as disseminated crystals in the claystone and shales. The products of zeolitization, dolomitization, and chloritization are rather widespread within the associated rock units of the trona

---

\*cahit.helvacı@deu.edu.tr

deposit, and the processes that formed these probably operated shortly after deposition or during diagenesis.

The Beypazarı basin was affected by an extensional tectonic regime during the Middle-Late Miocene period. This extensional regime became a single-directional compressional regime during the Late Miocene–Early Pliocene period. The sediments associated with the trona, lignite, and bituminous-shale deposits formed in fluvial, lacustrine, and playa-lake (perennial and ephemeral) environments. The Beypazarı basin is mainly filled by clastic materials and the penecontemporaneous products of adjacent volcanic activity that was centered northeast of the basin. The most likely sources of Na for the formation of the trona and other sodium-carbonate salts were thermal springs, the tuffs interbedded with the sediments, and the extensive Neogene volcanic rocks interfingering with sedimentary rocks in the northeastern part of the basin.

## PREFACE

This field guide has been prepared for the field excursion to the Beypazarı trona basin during the meeting of “Tectonic Crossroads: Evolving of Orogens of Eurasia-Africa-Arabia” (4–8 October 2010) held in Ankara, Turkey, on Wednesday, 6 October 2010. The aim is to set forth the stratigraphy, tectonics, and ideas concerning basin formation of the Beypazarı trona deposit, the world’s second largest deposit after that of Green River, Wyoming, USA.

The guide is divided into two sections. The first section gives general information on the tectonics, stratigraphy and mineralogy of the trona deposit. The second part deals specifically with the field-trip stops. All stops mentioned in the guidebook can be reached using a normal field vehicle. Similar text has been originally published by the Chamber of Geological Engineers for the 63rd Geological Congress of Turkey (Excursion Series–7; ISBN: 978-9944-89-956-7). The present text is a revised version.

## INTRODUCTION

A sedimentary sequence ~1200 m thick, ranging in age from Middle to Late Miocene, crops out in the Beypazarı-Çayırhan district (Fig. 1). From the standpoint of stratigraphy, sedimentology, and tectonic evolution, the Beypazarı basin differs from other parts of central Anatolia, as it does by the presence within it of economic resources, such as lignite, bituminous shale, trona, Na-sulfates, gypsum, and clay minerals.

Birön et al. (1979), Narin (1980), and Yağmurlu et al. (1988), as well as other previous workers, studied the geology of the lignite and bituminous shale and other economic resources of the basin.

The Beypazarı Neogene basin is filled mainly by fluvial, lacustrine, and volcano-sedimentary rocks. The Neogene sedimentary sequence in this basin has been divided into eight formations (İnci et al., 1988; Helvacı and İnci, 1989). In the region between Beypazarı and Nallıhan, geological maps have been prepared and stratigraphic sections measured at different loca-

tions in order to determine the distribution of rocks units, facies changes, and tectonic features of the basin, as well as to ascertain the geological setting of the trona deposit.

The Neogene Beypazarı basin is limited to the north by the western Pontide mountain belt. This part of the Pontides comprises metamorphic, volcanic, and sedimentary rocks that are Paleozoic to Tertiary in age (Kalafatçioğlu and Uysallı, 1964; Ketin, 1966; Saner, 1979; Varol and Kazancı, 1981). The Middle Sakarya Massif consists mainly of metamorphic, acidic-plutonic, and ultrabasic rocks and occurs to the south of the Beypazarı basin (Saner, 1979). The Tertiary volcanic rocks are distributed in the northeastern part of the basin between the Beypazarı and Kızılcahamam areas (Öngür, 1977) (Fig. 1). The pre-Neogene sedimentary rocks limit the Neogene basin from the west and vary from Paleocene to Eocene in age.

The trona deposit, located 250–300 m below the surface, was discovered incidentally in the summer of 1982 by the general directorate of the Mineral Research and Exploration (MTA) while carrying out a drilling project on lignite deposits. An extensive exploratory drilling program was undertaken by MTA during the period 1983–1985 on behalf of the Etibank Company. Proven trona reserves are 210 million metric tonnes, and total reserves are estimated as 240 million metric tonnes (Nasün-Saygılı et al., 1974; Kayakıran et al., 1986; DüNDAR, 1988; Helvacı et al., 1989; Helvacı, 1998, 2001; Onargan and Helvacı, 2001). The Beypazarı trona deposit is the world’s second largest trona deposit after the Green River deposit, Wyoming, USA. In addition, there are ~400 million metric tonnes of lignite, 340 million metric tonnes of bituminous shale, and 1 million metric tonnes of Na-sulfate in the Beypazarı basin (Helvacı and İnci, 1989; Gündoğan and Helvacı, 2001; Orti et al., 2002).

## STRATIGRAPHY

The rock units of the study area are divided into two main groups: pre-Neogene basement rocks and Neogene rock units (Figs. 2 and 3). The pre-Neogene basement rocks are Paleozoic to Eocene in age and comprise metamorphic, plutonic, volcanic

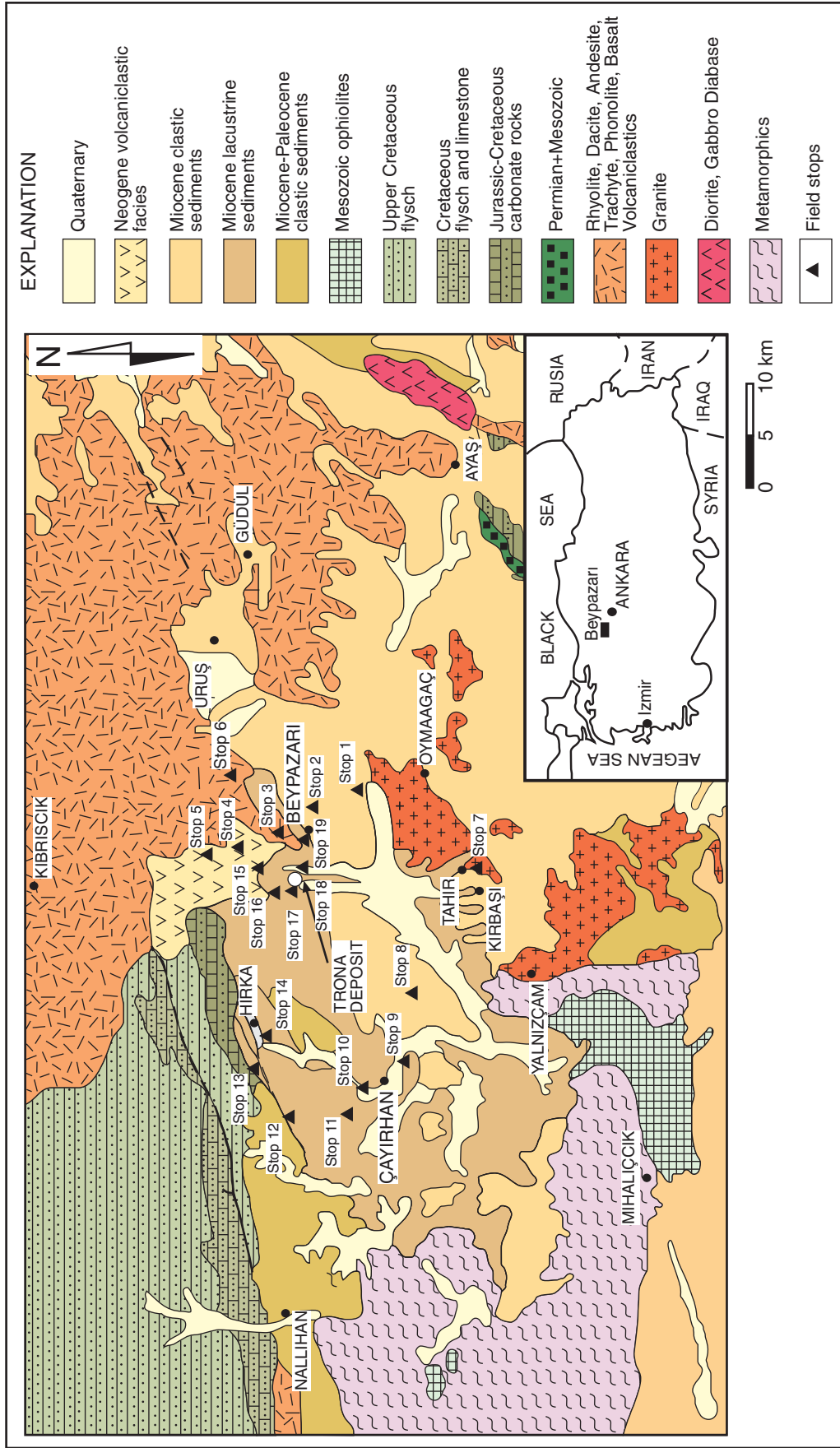


Figure 1. Locality and geological setting of the Beypazari basin and adjacent areas. Also shown are field stops.

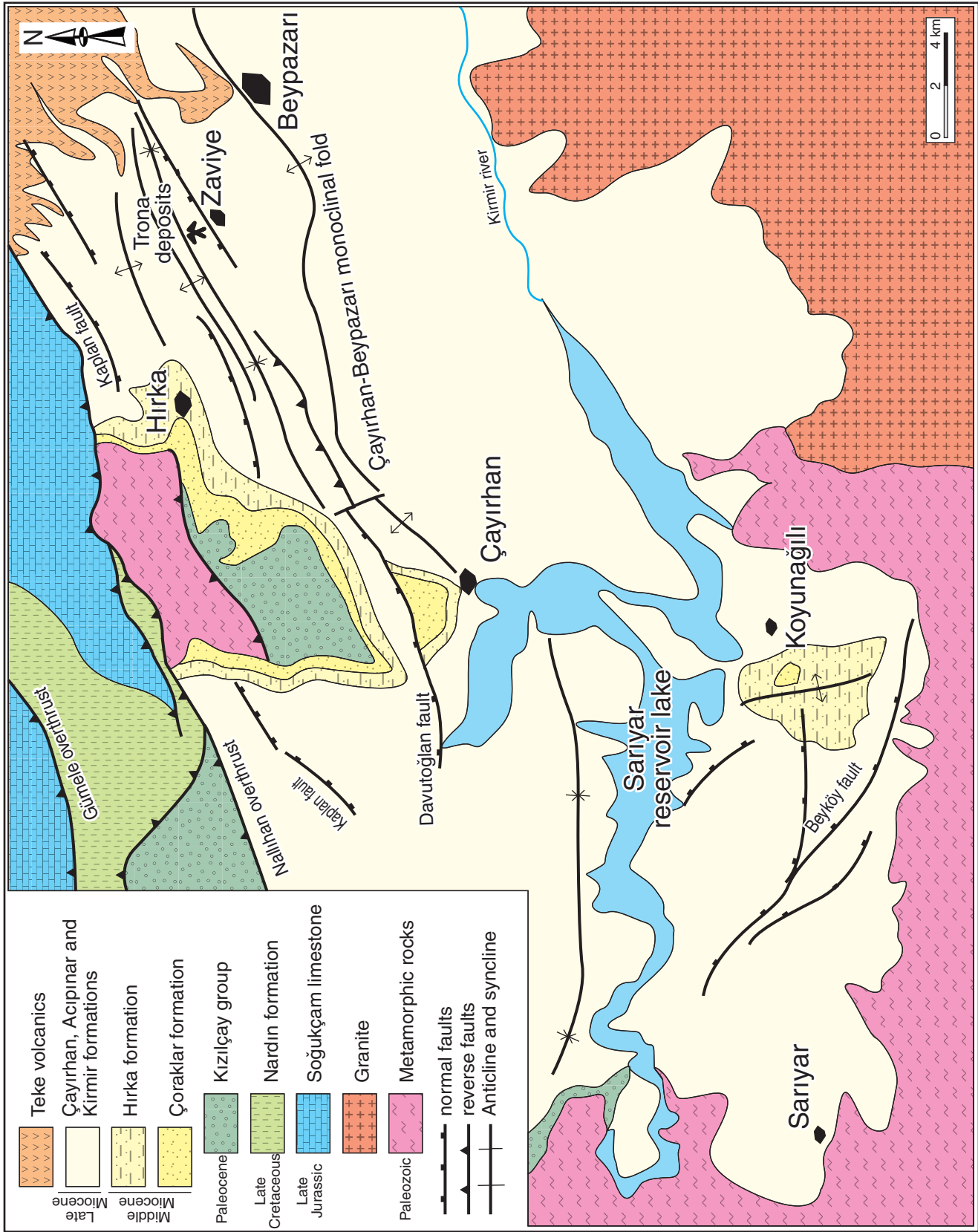


Figure 2. Geological and structural map of the Beypazarı basin.

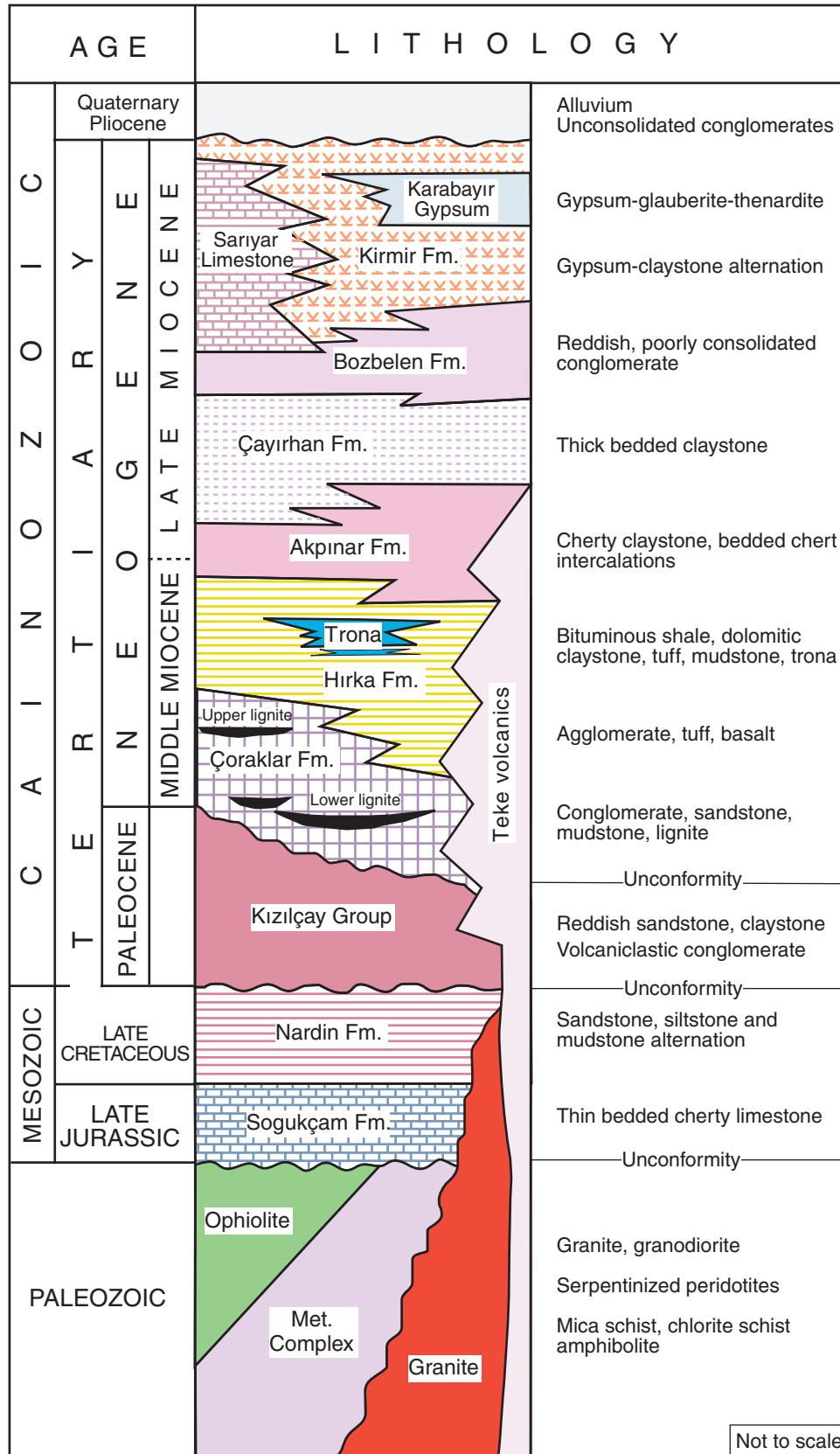


Figure 3. Stratigraphic column section of the Beypazarı trona basin.

and sedimentary rocks. The Neogene sedimentary units generally consist of clastic, clayey, calcareous, bituminous, evaporitic, and silicified sediments.

The Neogene sedimentary sequence is divided into seven formations (Figs. 2 and 3); in ascending order, these are: the Çoraklar, Hırka, Akpınar, Çayırhan, Bozbelen, and Kirmir formations, plus the Sariyar Limestone and the Teke volcanics (İnci et al., 1988; Helvacı and İnci, 1989).

### Pre-Neogene Rock Units

The pre-Neogene basement comprises chiefly metamorphic rocks, granite, ultramafic rocks, the Soğukçam Limestone, and the Kızılçay Group, ranging in age from pre-Permian to Middle Eocene.

The oldest rocks observed in the study area belong to the Paleozoic metamorphic rocks, which comprise mica schist, chlorite schist, amphibole schist, quartzite and marble (Altınlı, 1976, 1977). Upper Cretaceous granitic rocks cut the Paleozoic metamorphic and early Cretaceous rocks and are overlain by the Paleocene Kızılçay group in the Beypazarı area. Granitic rocks crop out over a wider area south of Beypazarı (Figs. 1 and 2). Aplite and pegmatite veins are widespread in the granites and strike NE-SW and NW-SE and dip to the south (Helvacı and Bozkurt, 1994). Table 1 gives chemical analyses of selected granitic rocks from the area.

The rocks generally designated as ultramafic rocks comprise mainly serpentinite, metabasite, red chert, and gabbroic rocks. The ultramafic rocks were thrust onto the metamorphic rocks along a tectonic contact during the Late Cretaceous.

The Jurassic rocks comprise thin-bedded, micritic, sparitic, and ammonitic fossiliferous limestones alternating with sandstone, shale, and chert layers, and were named the “Bilecik

Limestone” by Altınlı (1973, 1976, 1977). The Bilecik limestone grades into a Lower Cretaceous limestone, named the “Soğukçam Limestone” by earlier workers. The Late Cretaceous sequence comprises turbiditic clastic rocks and rests concordantly on Lower Cretaceous limestones (Önal et al., 1988).

The Paleocene sequence consists mainly of reddish and grayish conglomerate, sandstone, siltstone, mudstone, thin-bedded limestone, and greenish to brownish volcanoclastic rock units in the region. These rock units were named the “Kızılçay Group” by Altınlı (1976, 1977) and Saner (1979). The Kızılçay Group was deposited within fluvial and lacustrine environments, and its total thickness exceeds 2000 m (Önal et al., 1988). Eocene rocks comprise limestones and sandstones having a total thickness of ~250 m due to extensive post-Eocene erosion. In the northern part of the area (Figs. 1 and 2), Jurassic and Cretaceous units have tectonic contacts with the other rock units, and are thrust to the south over the Paleozoic metamorphic complex and the Paleocene clastic rocks (Altınlı, 1976; Yağmurlu et al., 1988).

### Neogene Rock Units

#### Çoraklar Formation

The sediments of the Çoraklar Formation comprise volcanoclastic conglomerates, sandstones, siltstones, and mudstones and were deposited in braided-meandering river and flood-plain environments. The lower lignite seam occurs in the lower part of the Çoraklar Formation and formed in channel-controlled swamps of a river system (Fig. 2). The upper lignite seam occurs in the uppermost part of the Çoraklar Formation, was deposited in a lake-margin mud-flat environment, and is overlain by the Hırka Formation along a sharp contact (Yağmurlu et al., 1988; Helvacı and İnci, 1989).

TABLE 1. WHOLE-ROCK ANALYSES OF MAJOR OXIDES AND SELECTED TRACE ELEMENTS IN GRANITES FROM THE BEYPAZARI BASIN

	1	2	3	4	5	6	7
<b>Oxide (wt%)</b>							
SiO <sub>2</sub>	57.60	74.97	65.04	52.64	59.17	65.35	67.52
Al <sub>2</sub> O <sub>3</sub>	17.59	12.33	16.28	18.38	21.67	15.75	14.96
Fe <sub>2</sub> O <sub>3</sub>	3.49	0.22	2.09	4.80	0.42	2.11	1.21
FeO	3.88	0.26	2.34	5.33	0.47	2.35	1.34
MgO	2.51	0.27	1.12	3.41	1.25	1.22	0.64
CaO	7.46	0.85	5.04	8.00	7.74	5.19	2.97
Na <sub>2</sub> O	3.00	3.27	3.54	2.96	7.0	3.32	3.55
K <sub>2</sub> O	2.71	4.95	4.29	2.28	0.3	3.97	3.8
TiO <sub>2</sub>	1.10	0.70	0.52	1.60	1.2	0.70	0.7
P <sub>2</sub> O <sub>5</sub>	0.30	0.19	0.15	0.30	0.2	0.20	0.2
LOI	0.57	0.42	0.33	0.69	0.23	0.39	0.55
TOTAL	99.64	99.87	100.41	100.39	99.63	100.55	97.44
<b>Elements (ppm)</b>							
Rb	75	333	134	62	8	126	72
Sr	509	61	728	410	676	633	610
Y	31	34	53	25	30	51	22
Zr	115	66	150	74	135	144	148
Nb	12	16	13	17	6	23	6

Note: LOI = loss on ignition.

Conglomerates are dominant in the lowermost part of the alluvial sequence of the Çoraklar Formation, which is continuous to the top as sandstone-mudstone alternations; also, channel-fill conglomerates occur locally in the uppermost part of the sandstone-mudstone sequence. Drilling information indicates that the thickness of this unit is ~150 m, increases from north to south, and reaches 250 m in the Çayırhan area. The clastic sediments of the Çoraklar Formation overlie the preexisting rock units along an angular unconformity (older than Neogene) and grade laterally into the Hırka Formation to the northeast (Figs. 3 and 4).

The conglomerates of the Çoraklar Formation are yellowish, moderately consolidated, poorly sorted, well drained, trough shaped, large scale (75–125 cm), and cross bedded and generally occur in fining-upward, graded beds. Medium-sized clasts range between 3 and 6 cm, and maximum sizes range from 10 to 12 cm. The conglomerates contain locally imbricated clasts, mudstone, and sandstone intercalations and rip-up clasts within the lower parts of the unit. Sandstones are locally trough shaped and cross bedded. Grains generally are angular to subrounded and are moderately to well sorted. Mudstones generally are light greenish, poorly bedded, and locally consist of siltstone, fine sandstone, and plant detritus. These features of the mudstones indicate well-drained swamp conditions in the fluvial environment.

Sedimentary structures include planar and trough cross bedding, parallel laminations, convoluted bedding, graded beds, and burrows. These sedimentary structures probably indicate a high- to mid-flow regime of a meandering-stream system. Field measurements of internal sedimentary structures indicate that the dominant transport directions were to the SE and SW. It is believed that the channel conglomerates were formed by lateral and vertical migration of mobile stream channels on the alluvial plain, derived from rocks of the western Pontides.

### ***Hırka Formation***

The Hırka Formation rests concordantly upon the upper lignite seam of the Çoraklar Formation and is composed mainly of mudstone, claystone, bituminous shale, trona, gray shale, calcareous shale, dolomitic limestone, siltstone, intraformational conglomerate, and tuff (Figs. 4 and 5). The Hırka Formation was apparently deposited in a playa-lake environment, and trona is deposited in the central part of that environment (Fig. 5). Claystone and mudstone were deposited in the playa or mudflat of the lake environment. Bituminous shales were deposited in a periodically expanding lake environment.

The Hırka Formation is transitional vertically and laterally with the underlying Çoraklar Formation. The total thickness of the Hırka Formation increases eastward and exceeds 300 m where the trona deposit occurs. The unit interfingers with the Teke volcanics along İnözü Dere to the NW of Beypazarı (Figs. 5 and 6).

The mudstone and claystone of the Hırka Formation are greenish and grayish, thick bedded, moderately consolidated, and include partially framboidal pyrite crystals. They grade locally into argillaceous siltstone, calcareous shale, or gray shale. The

bituminous shales are typically dark grayish to brownish black, thin bedded, and finely laminated (Fig. 5). The organic-carbon content is ~13%, and the upper calorific values range between 600 and 1140 kcal/kg (Birön et al., 1979). The dolomitic limestones are usually thin (1–3 m), gray to whitish, micritic, and partially silicified. The intraformational conglomerate is whitish, micritic, partially silicified, thick bedded, well consolidated, clay and mud supported, and composed mainly of angular tuff and bituminous-shale gravels, cobbles, and minor boulders. The conglomerate interfingers with the other rock associations of the Hırka Formation. The tuffs are generally whitish, thin and thick bedded, locally fragmented, and alternating with the other rock components of the unit. A tuff sample interbedded in the Hırka Formation yields a  $21.5 \pm 0.9$  Ma age determination by the K-Ar method; the K-Ar age dating method used in this study was set forth by Damon et al. (1983). Some sections of the unit to the north of Beypazarı include thin (1–2 m) basalts, sills, and silicified wood fragments (Fig. 5).

The trona deposit is within the lower part of the Hırka Formation and alternates with bituminous shale and claystones (Figs. 5 and 6). The trona deposit covers ~8 km<sup>2</sup> around Çakılöba village, according to MTA drill data. The trona beds were deposited within a 70- to 100-m-thick zone as lenticular bodies and grade laterally into and interfinger with mudstone, claystone, and bituminous shales at the edges of the trona deposit (Fig. 5; Helvacı, 1998).

### ***Akpınar Formation***

The Akpınar Formation comprises an alternation of silicified limestone, chert, tuff, claystone, and mudstone. The lower and uppermost parts of the unit are represented by lower and upper limestone members, whereas the middle part is represented by an alternation of the green claystone and bedded cherts. At the type section, the Akpınar Formation is 150 m thick and has a gradational contact with the underlying Hırka Formation. The Akpınar formation grades into the Çayırhan Formation from east to west (Figs. 4 and 6).

### ***Çayırhan Formation***

The Çayırhan Formation consists mainly of greenish claystone, mudstone, marl, and local sandstone. Mudcracks, salt crystals, and burrows are dominant sedimentary structures of the Çayırhan Formation. This sequence contains playa-type lacustrine and mud-flat facies. The Çayırhan Formation varies in total thickness from 150 to 300 m and rests conformably (but with a sharp contact) upon the Akpınar Formation (Figs. 4 and 6).

### ***Bozbelen Formation***

The Bozbelen Formation consists mainly of reddish conglomerate, sandstone and mudstone, indicating an alluvial-fan environment. The thickness of the formation increases from south to north and reaches 100 m in the marginal parts of basin. The Bozbelen Formation rests conformably on all older rock units (Figs. 4 and 6).





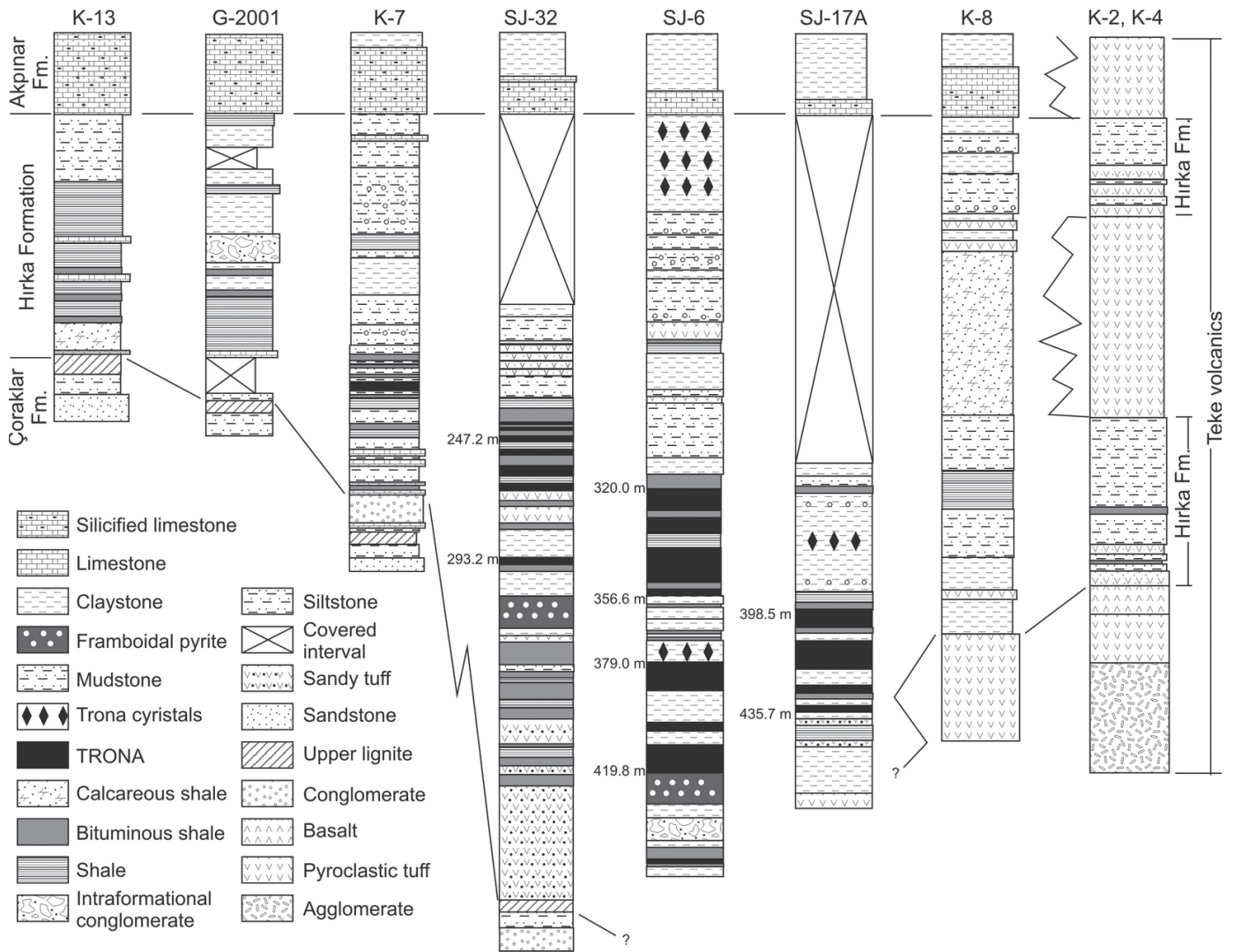


Figure 5. Type and reference sections, along the NE-SW direction and stratigraphic relations of the Hirka Formation.

**Kirmir Formation**

The Kirmir Formation consists of gypsiferous green claystone, Na-sulfates, and bedded gypsum, and its distribution is widespread in the basin. The Kirmir Formation occurs in the Beypazarı basin within the uppermost part of the Miocene sedimentary sequence and contains numerous evaporite horizons; in ascending stratigraphic order, these are a gypsiferous claystone facies, a thenardite-glauberite facies, a laminar gypsum facies, and a crystalline gypsum facies (Yağmurlu and Helvacı, 1994; Gündoğan and Helvacı, 2005; Orti et al., 2002). The unit is laterally and vertically gradational with the Sarıyar Limestone and Bozbelen Formation (Figs. 4 and 6).

**Sarıyar Limestone**

The Sarıyar Limestone is composed mainly of whitish, thick-bedded, and micritic lacustrine limestone. The thickness of

the unit increases from east to west and reaches up to 150 m in the area around the Sarıyar Dam (Figs. 4 and 6).

**Teke Volcanics**

The Teke volcanics are widespread in the area NE of Beypazarı and Kızılcahamam. These volcanic rocks consist of alternating pyroclastic breccia, tuff, and andesitic and basaltic lavas and agglomerate, and are of Early Eocene to Late Miocene age (Figs. 4 and 6). The lower and middle parts of the Beypazarı Miocene sequence interfinger with the Teke volcanics, comprising pyroclastic tuff and basalt units. The Beypazarı trona deposit accumulated in a narrow area near this zone of interfingering. The İnözü Tuff is composed of whitish, thick to massive, alternating beds of crystal and lithic tuff, reworked tuff, and volcanoclastic conglomerate. The agglomerates are present below the tuffs in some localities.

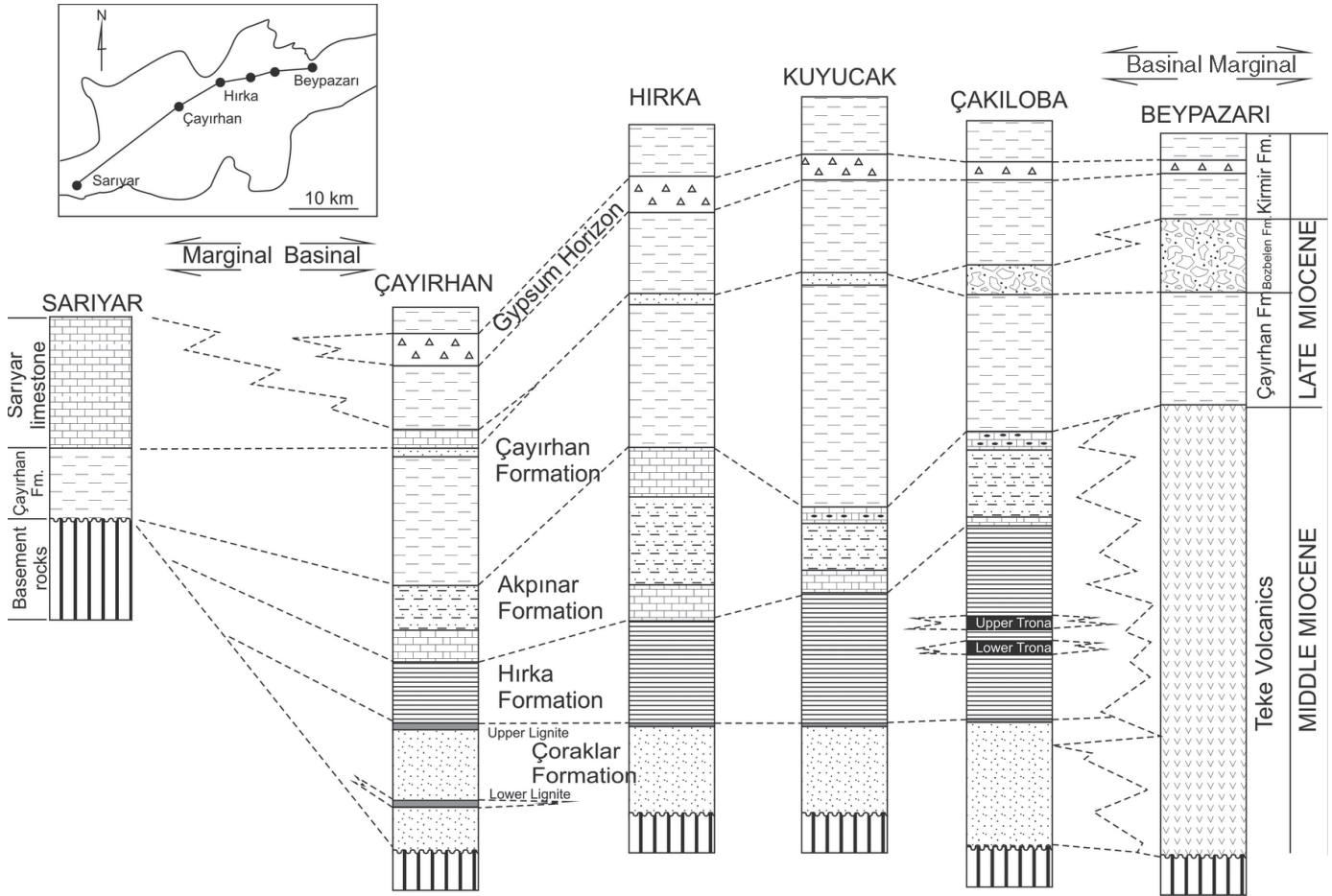


Figure 6. Correlation of the rock succession in different parts of the Beypazari Miocene basin.

The Adaviran Basalt consists of black lava flows and minor amounts of tuff. The total thickness of the lava flows exceeds 300 m. The unit covers a wide area around Adaviran village.

The Beypazari Miocene sequence that is exposed in the eastern part of the basin, where interfingering with the Teke volcanics, is thicker than the sequence in the western part of the basin; the trona deposit occurs in this transition zone. The tuff interlayers and the grade of silicification of the rocks increase toward the Teke volcanics, which form the southwestern edge of the volcanic rocks described by Öngür (1977) as an alternation of the pyroclastic breccia, tuff, and andesitic and basaltic lavas of the Kızılcahamam (Ankara) district. The results of chemical analyses of the Teke volcanics are given in Table 2.

### STRUCTURE OF THE BEYPAZARI BASIN

The Beypazari Miocene basin extends approximately in an E-W direction and is limited by growth faults to the north and south. The growth faults in the northern part of the basin have high displacements resulting from stepwise structural features,

which occur mainly at the contact between the Miocene sediments and the basement rocks. The growth faults at the southeastern margin of the basin have small displacements and only developed as an asymmetric depression in the first phase, based on analysis of tectonic features. The fluvial and lacustrine sediments were deposited in an asymmetric depression during Miocene time and were controlled by the growth faults at the northern margin (Figs. 2 and 7).

The Beypazari basin was affected by an extensional tectonic regime during the Middle-Late Miocene. Related to this tectonic regime, the NE-SW-trending normal faults developed, and sedimentation in the basin was controlled by the faults throughout the Miocene Epoch. The stratigraphic and sedimentologic features of the sequence and the placement of the faults indicate a half-graben type of depressional basin. This extensional regime became a single-directional compressional regime during the Late Miocene–Early Pliocene. Under the influence of this new tectonic regime, the Miocene rock units were folded, and the rocks of the northern margin of the basin were thrust over basement rocks (Fig. 7). The compressional forces probably originated from the

TABLE 2. WHOLE-ROCK ANALYSES OF MAJOR OXIDES AND SELECTED TRACE ELEMENTS IN THE TEKE VOLCANICS FROM THE BEYPAZARI BASIN

	B6-2	B6-3A	B6-5	B6-6	B6-8	B6-10	B63	B67	B79	B82
<b>Oxide (wt%)</b>										
SiO <sub>2</sub>	66.30	65.73	65.92	65.21	66.79	67.00	44.68	66.75	58.54	62.10
Al <sub>2</sub> O <sub>3</sub>	16.05	16.76	16.04	16.14	15.41	15.20	15.46	16.13	16.27	16.60
Fe <sub>2</sub> O <sub>3</sub> <sup>T</sup>	3.18	2.59	3.18	3.47	3.37	3.22	8.11	2.95	5.91	5.26
MgO	1.34	1.26	1.82	1.97	1.56	1.83	5.55	1.55	3.70	1.83
CaO	4.36	4.86	4.82	5.28	4.38	4.67	10.20	4.35	5.63	4.98
Na <sub>2</sub> O	3.55	4.02	3.27	3.48	3.49	3.31	5.09	3.38	4.42	4.28
K <sub>2</sub> O	3.95	3.56	4.19	3.61	4.23	4.02	1.50	4.20	2.02	1.87
TiO <sub>2</sub>	0.34	0.29	0.37	0.42	0.38	0.37	1.23	0.32	1.06	1.05
P <sub>2</sub> O <sub>5</sub>	0.29	0.32	0.31	0.34	0.29	0.30	0.74	0.28	0.44	0.35
MnO	0.09	0.06	0.09	0.08	0.09	0.09	0.09	0.08	0.07	0.06
H <sub>2</sub> O	0.54	0.53	0.00	0.00	0.00	7.23	7.23	0.00	1.93	1.62
TOTAL	99.99	99.98	100.01	100.00	99.99	99.88	99.88	99.99	99.99	100.00
<b>Elements (ppm)</b>										
Rb	152	121	150	138	158	162	31.84	165	63	61
Sr	613	667	538	549	590	497	1007	585	592	552
Y	25	19	19	21	24	23	18	20	22	18
Zr	109	88	107	94	118	102	143	101	239	206
Nb	14	11	8	9	13	12	22	10	22	18

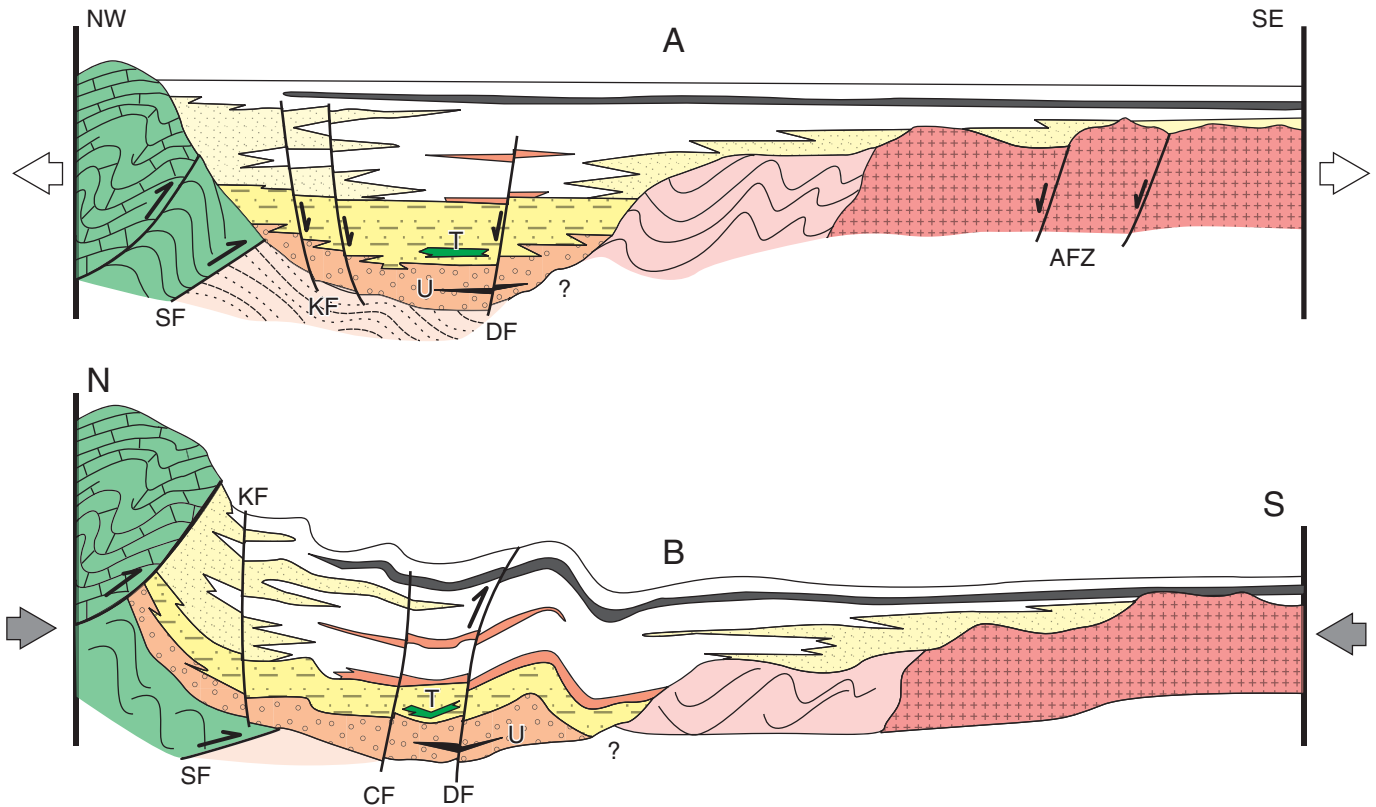


Figure 7. Tectosedimentary evolution of the Beypazari Miocene basin: (A) Miocene extension phase. (B) Post-Miocene compressive phase. Big dots—lower alluvial facies; small dots—upper alluvial facies; dashed lines—lithofacies of the Hirka Formation; U—upper lignite; T—trona; diagonal strips—carbonate rock; white tone—green claystone lithofacies; dark line—evaporite lithofacies (sulfates); KF—Kaplan fault; DF—Davutoğlu; SF—Sekli fault; AFZ—Ayaş fault zone; CF—Çömlekçe fault.

oppositional movement of the strike-slip North Anatolian Fault against the passive block of the Eskişehir Fault and the Middle Sakarya Massif (Figs. 2 and 7).

The extensional tectonic regime affected this region during the Middle Miocene. A high degree of subsidence occurred under the influence of this extensional regime, thus localized faults (as growth faults) developed at the southern margin of the basin in the Early and Middle Miocene. In addition, intraformational breccias derived from the southern part of the basin and small synsedimentary folds (overturned to the north) are observed in the Hirka Formation in the Çayırhan underground coal mine. These occurrences are significant in so far as they indicate the beginning of synsedimentary tectonism (that coincided with sedimentation in the southern part of basin during deposition of the Hirka Formation).

Asymmetric anticlines, synclines and monoclines are abundant in the Beypazarı basin, and their axes are predominantly E-NE trending. The fold axes trend E-W and NE-SW, and the dips of the limbs range between 15 and 50 degrees. These folds were generally developed in the northern part of the basin. The high-angle limbs of the folds and monoclines usually dip toward the south, and the northern limbs are low-angle and locally are nearly horizontal. The Beypazarı-Çayırhan monoclinial fold is the largest fold of the region and extends 30 km in an NE-SW direction (Figs. 2 and 7). The southern limb of monoclinial fold is high-angle, and locally the dip reaches 70 degrees. The overthrust faults, monoclines, and other fold axes parallel each other. The main structural elements of the study area include overthrusts, high-angle reverse faults, normal faults, and predominantly monoclinial and asymmetrical folds (Fig. 2). Locally, conjugate faults cut these fold systems obliquely. Geometrical features of these folds and faults indicate that compressional forces influenced the region from north to south after Miocene sedimentation. The compressional forces resulted from movement along the North Anatolian Fault and partly are a result of the passive aspect of the Middle Sakarya Massif and granitic plutons, which limit the Beypazarı basin to the south (Yağmurlu et al., 1988; Helvacı and İnci, 1989) (Figs. 1, 2 and 7).

The normal faults trend E-W and NE-SW and dip both to the north and south at angles ranging between 50 and 70 degrees. One of these normal faults is the Zaviye fault, which is observed in the south-central part of the basin and trends roughly NE-SW. The trona deposit of the basin is bounded on the south by this fault. N-S-trending strike-slip faults occurring in the area obliquely cut the normal- and reverse-fault systems. The rock units of the study area are affected by tensional and compressional tectonic forces. Some of the pre-Neogene normal faults have probably been transformed to high-angle reverse faults and overthrusts under the effects of compressional forces which prevailed during the Neogene Period. The strike-slip faults observed in the Neogene basin might also have been produced by these compressional stresses. All facies in the northern part of the basin were folded and faulted by compressional tectonic forces in the Late Miocene during movement along the North Anatolian Fault (Figs. 2 and 7).

## FACIES ANALYSIS OF THE BEYPAZARI MIOCENE SEQUENCE

Depositional features of the sedimentary-rock units are presented in Figures 2 and 4. Three major facies, including different lithofacies, have been defined in the Beypazarı basin. These facies are: (1) lower alluvial facies, (2) upper alluvial facies, and (3) lacustrine facies. In general, gray to whitish volcanic conglomerate, sandstone, and greenish siltstone and mudstone beds characterize the lower alluvial facies, and reddish conglomerate, fine-grained sandstone, and mudstone beds characterize the upper alluvial facies. Gray to brown shale, bituminous shale, green claystone, carbonate rocks, bedded chert, trona, and gypsum beds comprise the lacustrine facies (Helvacı and İnci, 1989; İnci, 1991). Figure 4 illustrates the distribution of the major facies and associated stratigraphic rock units as determined in measured sections and drill holes.

The lower alluvial facies is dominantly characterized by volcanic sandstone and green siltstone beds (Çoraklar Formation) exposed to the north of Çayırhan town (Figs. 2 and 4). The lignite deposits of the Çayırhan district occurred in the lower and upper parts of this facies. The northeastern end of the facies is represented by volcanoclastic rocks that were derived from the Teke volcanics.

The rock units of the lower alluvial facies were deposited in alluvial fans and subenvironments of the braided-river system during the first phase of sedimentation, which began in the late Middle Miocene (Fig. 4). The lower lignite seams developed in well-drained swamps, and the lignite distribution was controlled by braided channels. Following deposition of the lower lignite, the basin was filled rapidly by volcanoclastic materials and flood sediments of the adjacent basement rocks. At the end of this sedimentation stage, the basin was occupied by a shallow lake surrounded by swamps and mud flats that were responsible for the upper lignite seams. The lignites indicate a widespread forest-moor environment with a moist, subtropical climate during this sedimentation phase.

The ~600-m-thick layer of green claystone and carbonate rocks cropping out in the basin represents the most extensive suite of the lacustrine lake facies (Fig. 4). The lower part of the lacustrine facies (Hirka Formation), including the trona and bituminous shale deposits, accumulated along the depositional axis, crossing the basin in a SW-NE direction.

The red conglomerate and fine-grained sandstone beds of the upper alluvial facies reach maximum thickness at the southwestern and northeastern margins of the basin. The thickness decreases toward the inner part of the basin, and the facies units fringe and intertongue with rocks of the lacustrine facies (Fig. 4). The facies is represented by red, poorly consolidated conglomerate NE of Beypazarı, and channel-form conglomerate and sandstone in the southwestern and northeastern parts of the basin, and grades laterally into green claystones of lacustrine facies (Fig. 4).

The red clastic rocks of the upper alluvial facies, green claystone, carbonate, and evaporite lithofacies of the lacustrine

system constitute the most extensive rock suite of the Beypazarı Miocene basin. These lithofacies were deposited, with varying thicknesses, at basin margins and in small, normal-fault–bounded subbasins. During this sedimentation phase, numerous rivers emptied into the subsiding basin, and they created a NE-trending perennial lake. The green claystone-bedded chert-tuff succession was deposited in this lake environment. During the initial and postdepositional phase of this rock succession, the lake was twice changed into a siliceous carbonate lake environment. During deposition of the olive-green claystones, the lake water was hypersaline and dried up periodically. The ripple marks and desiccation cracks in these claystones indicate drying of the lake several times.

The upper part of the green claystone lithofacies is represented by lacustrine carbonates in the southwestern part of the basin. Preliminary investigations suggest that these carbonate rocks were deposited in a saline-alkaline lake environment. The salinity of the lake increased during the Late Miocene and the lake became an extensive saline lake surrounded by a saline mud flat (Fig. 4). The thick gypsum and thin glauberite and thenardite layers were deposited in this environment (Gündoğan and Helvacı, 2001; Orti et al., 2002). Outlines of the facies relationships and distributions of the lithofacies components of the three major facies assemblages are shown in Figure 4 (Helvacı and İnci, 1989; İnci, 1991).

## TRONA DEPOSIT

### Structure of the Deposit

The trona deposit is associated with the Hırka Formation and alternates with bituminous shale, dolomitic claystone, and intraformational conglomerate (Fig. 5). According to the drill-hole data, 33 trona beds with thicknesses ranging from 40 cm to 2 m were deposited within a 70–100-m-thick zone of the Hırka Formation.

Based on borehole data, it is estimated that the areal extent of the upper trona horizon is ~8 km<sup>2</sup>, whereas the areal extent of the lower trona horizon is ~5.5 km<sup>2</sup> to the north of Zaviye village. The trona beds were deposited as two lensoidal bodies within a 70–100-m-thick zone in the lower part of the Hırka Formation (Fig. 8). A total of 33 trona beds are known—16 in the lower trona lens, and 17 in the upper lens. The total thickness of the lower trona horizon ranges between 40 and 60 m, and the total thickness of the upper trona horizon is ~40 m. Most of the trona beds contain brownish organic matter, pyrite, dolomite, and thin partings of normal sediment, all of which indicate that these beds were chemical deposits laid down on the lake floor during very low or ephemeral stages of the perennial saline lake. The interval between the lower and the upper trona horizons varies from 30 to 35 m. The total thickness of the trona beds in both lenses ranges between 21 and 34 m in the central parts, and between 2.50 and 12 m in the marginal parts of the ore bodies. The thickness of individual trona beds in both trona horizons ranges usu-

ally between 0.4 m and 2 m, but in extreme cases varies between 2 and 3 cm to 11.50 m. Seventeen of these beds are considered to be significant because of their definite thicknesses, in so far as they are significant for correlations. The isopach contours of both trona horizons are restricted by the Zaviye fault (Figs. 9 and 10).

The lower trona horizon occurs between the Zaviye and Çakıloba villages and has an elongated lensoidal shape that is oriented NE-SW. It is bounded by the Zaviye fault to the south (Fig. 9). In many places, the thickness of the lower trona horizon varies over short distances, as noted in the drill holes. Eight trona beds out of 16 are significant because of their thicknesses and their areal extents. Changes in the lateral thickness of the lower trona horizon are likely related to the paleolake topography and geochemical conditions of the depositional environments. In many places, this lower trona zone contains brownish claystone on top of the trona and bituminous shale.

The upper trona zone has nine significant trona beds, and three of these beds formed when the basin had its largest areal extent; they are also the thickest and most uniform of the beds. The average thickness of the upper trona horizon is 12 m. The upper trona horizon was deposited under more stable environmental conditions than those that affected the lower trona horizon. Structural contour maps of the lower and upper trona horizons are given in Figures 11 and 12. To the north of the Zaviye fault, approximately NE-SW–trending synclines and anticlines are present (Fig. 11).

The Zaviye fault, which appears to have acted as a growth fault during deposition of the trona deposit and associated rocks, formed as a result of the extensional tectonic regime that affected this area during the Early and Middle Miocene. The synclinal and anticlinal structures occurring in the trona field developed under the influence of compression that resulted from the movement along the North Anatolian Fault during the Late Miocene–Early Pliocene. The lower and upper trona horizons have been affected by asymmetrical folding. In addition, these types of fold systems suggest that the compressional forces operated from north to south during and/or after trona deposition. On the structural contour map of the upper trona horizon, a NW-SE–trending monoclinical fold with a high-angle flank dipping to the south is observable near Çakıloba village (Fig. 12).

The central part of the trona deposit is generally thicker than its marginal parts. The trona beds grade laterally into dolomitic mudstones and claystones toward the edges of the basin. The subsurface position, lateral gradation, lateral thickness variations, and the stratigraphic relations between the lower and the upper trona zones and the associated rock units are shown on Figures 8, 9, and 10.

### Mineralogy

Minerals from the Beypazarı trona deposit were identified by direct-recording X-ray diffractometric analysis using standard-powder and oriented-sample techniques. The predominant saline mineral of the saline beds is trona; minor amounts of nahcolite

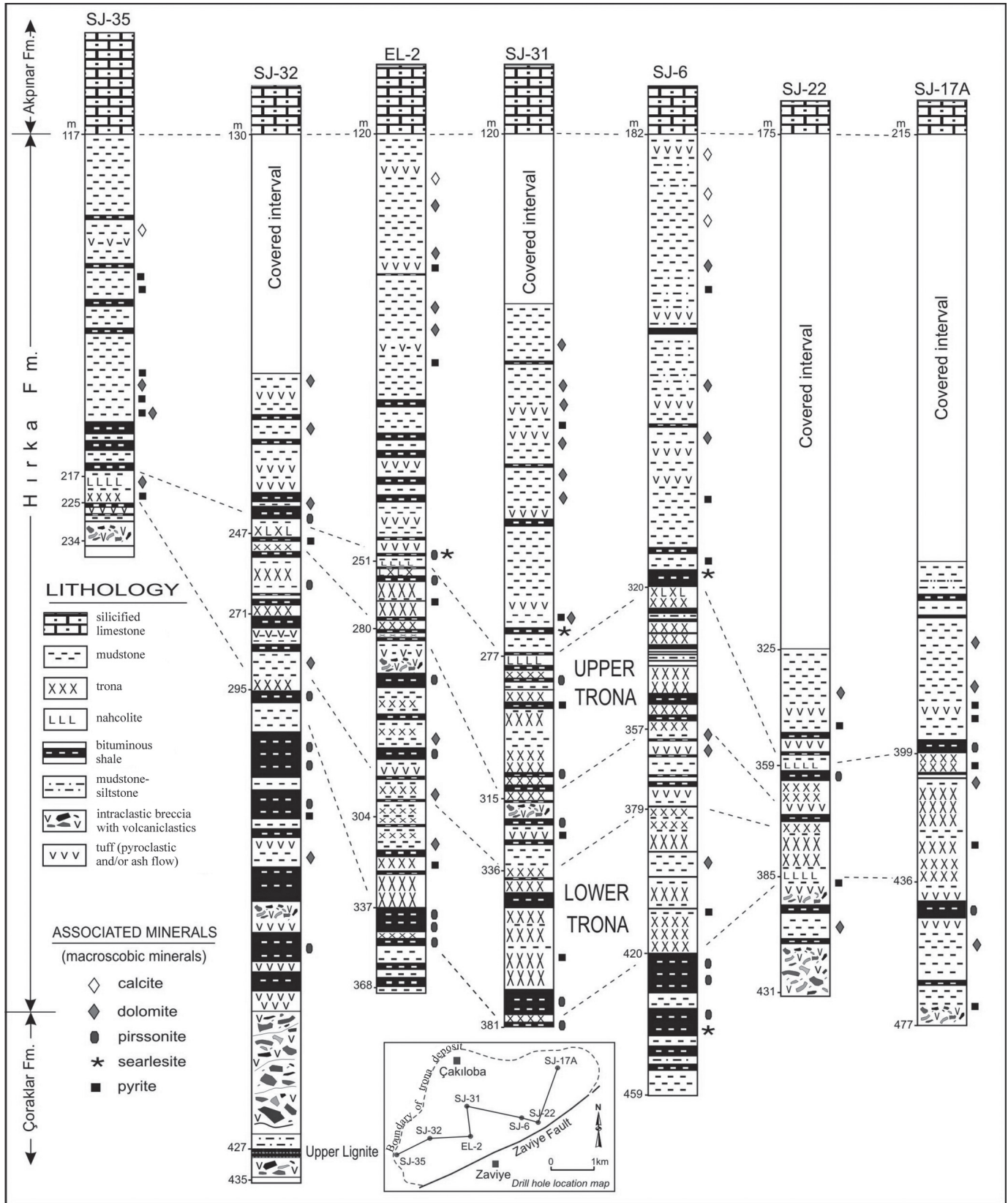


Figure 8. Correlation of lower and upper trona horizons in drill holes along the northeast and southwest direction, Beypazarı trona deposit.

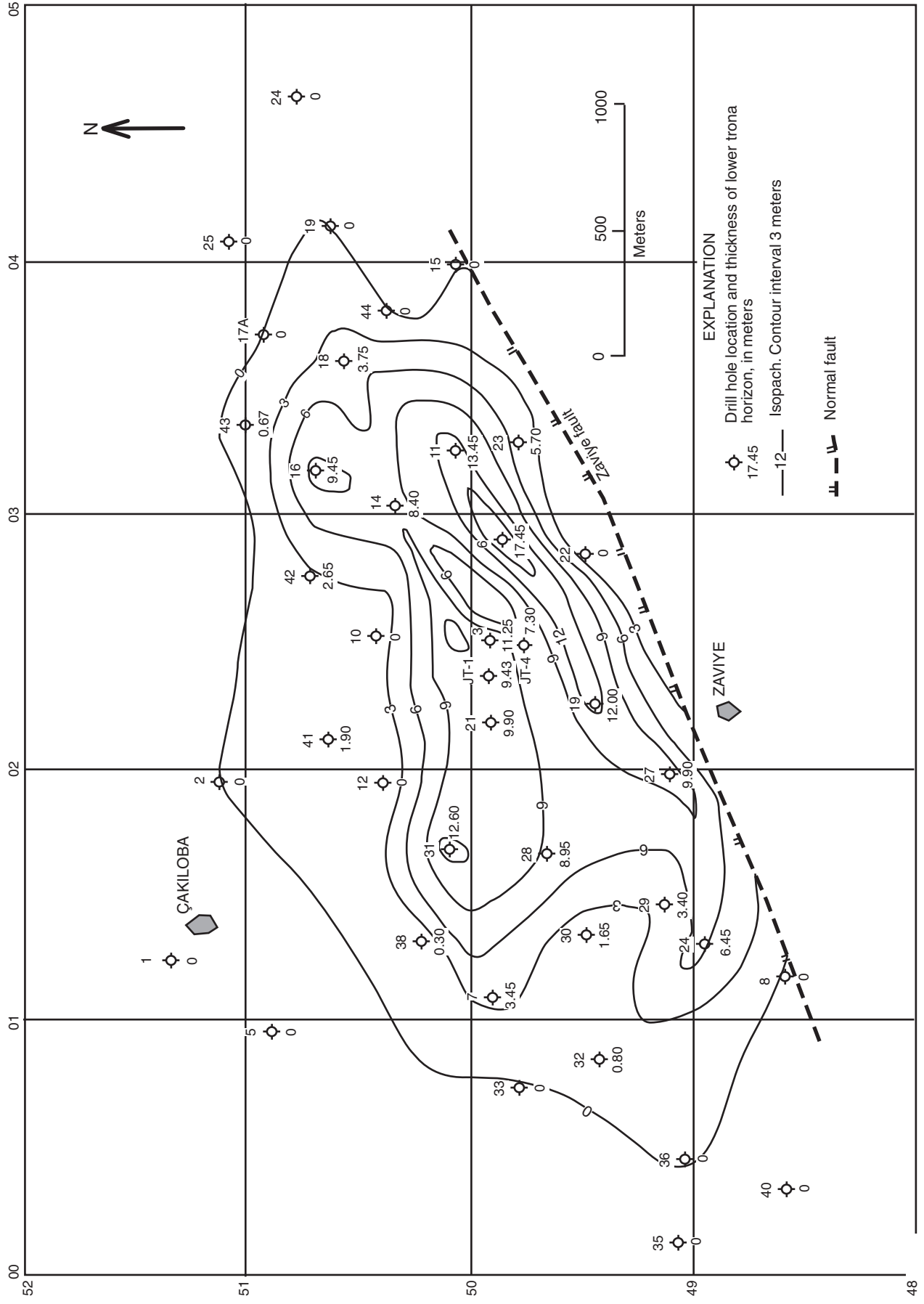


Figure 9. Isopach map of the lower trona horizon, Beypazarı trona deposit.

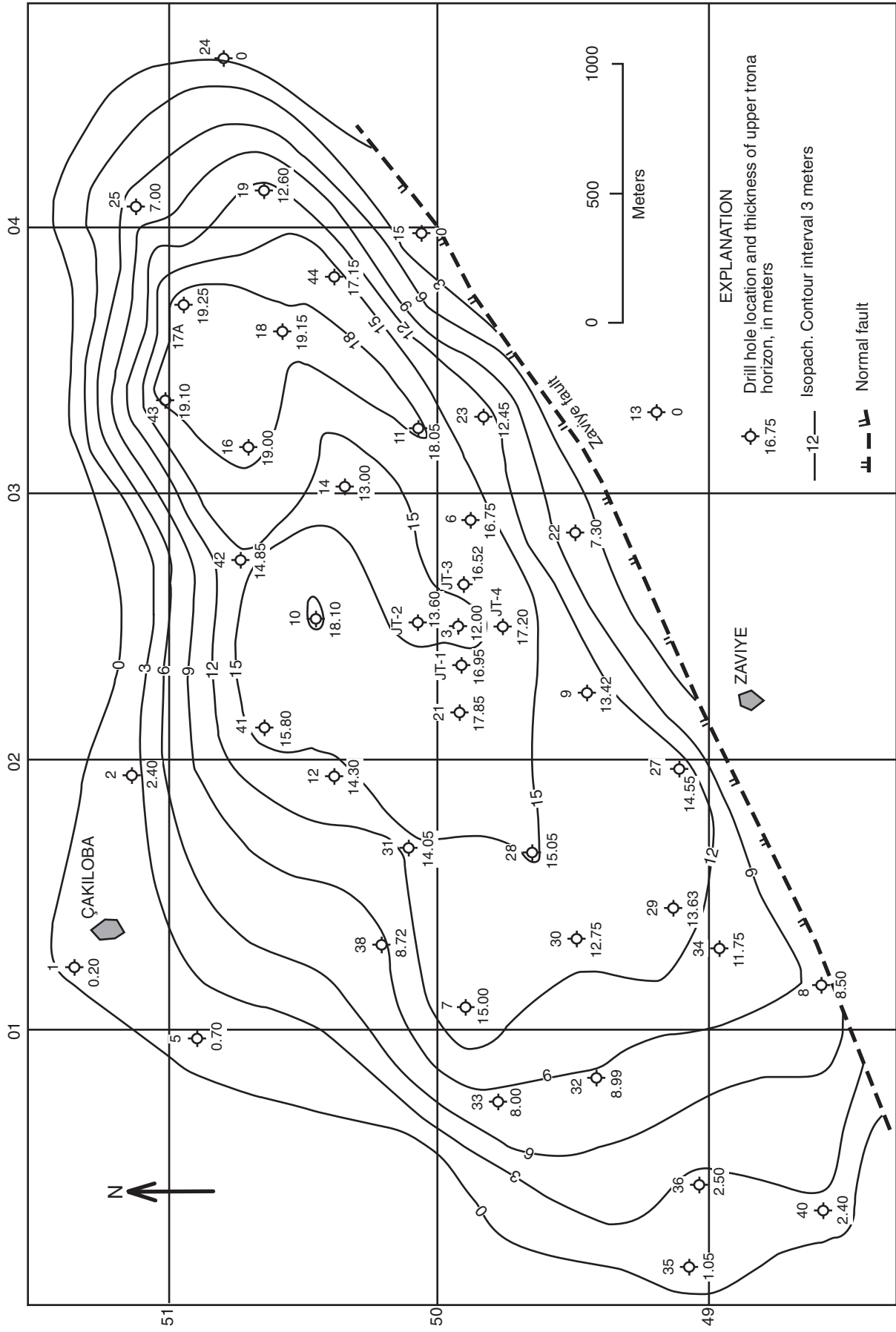


Figure 10. Isopach map of the upper trona horizon, Beyazarı trona deposit.



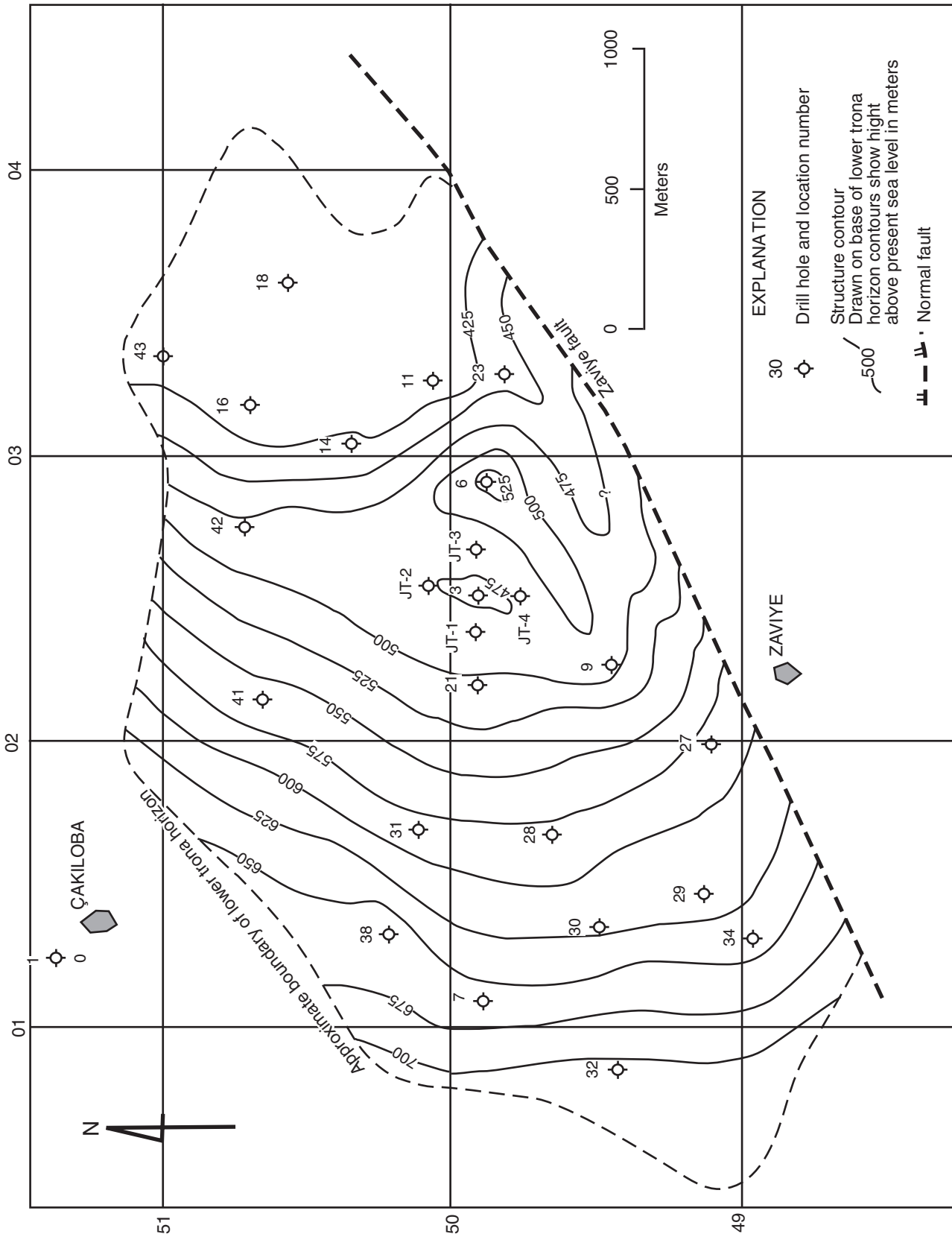


Figure 11. Structure contour map of the lower trona zone, Bey pazari trona deposit.

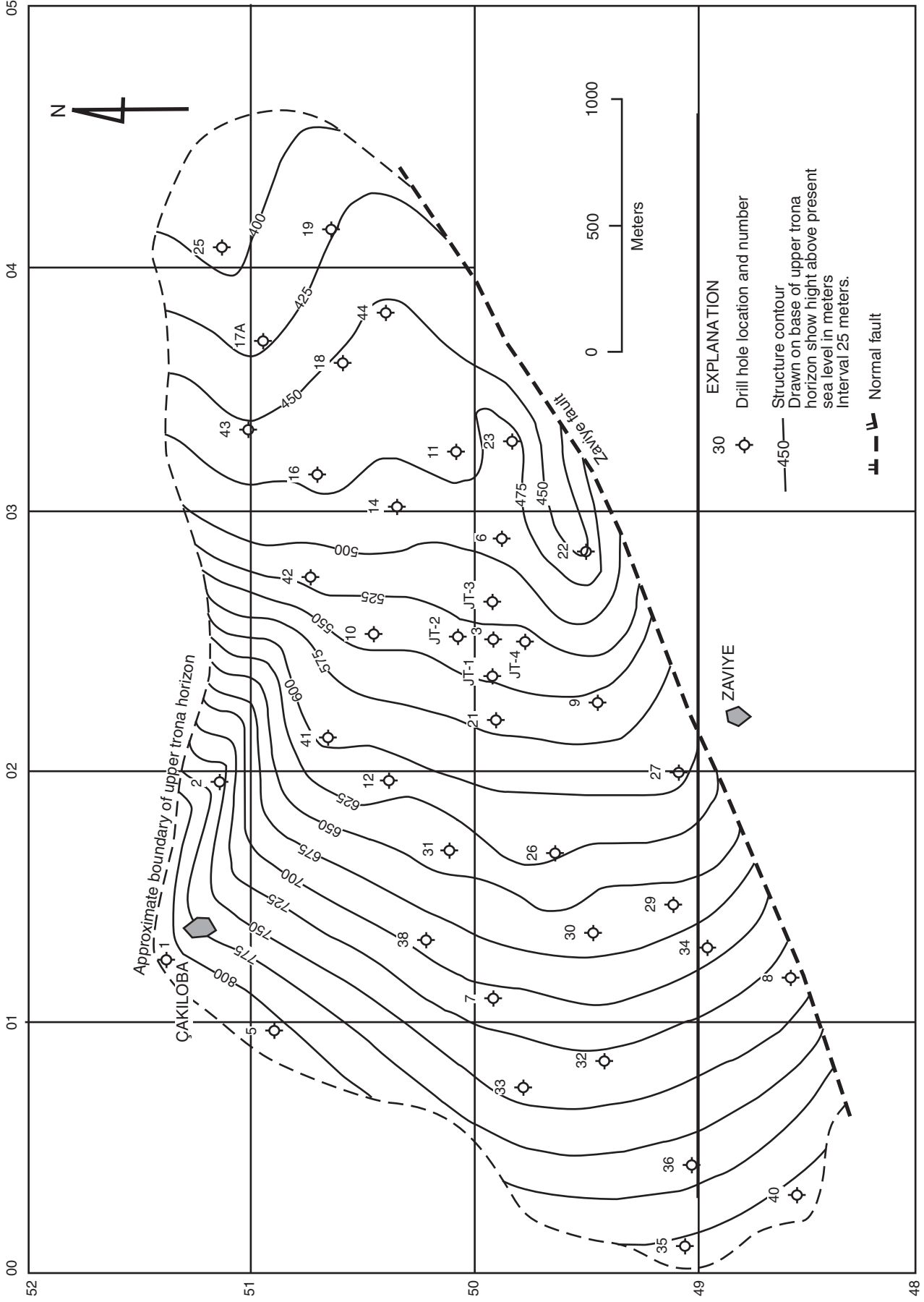


Figure 12. Structure contour map of the upper trona zone, Beypazarı trona deposit.

are found in the marginal and upper parts of the trona deposit (Fig. 8). Trace pirssonite and thermonatrite occur locally within the deposit (Table 3). Neither shortite nor halite appears to be present. Trona and dolomite are associated throughout the deposit. Clay minerals (mainly smectite and illite), zeolite, feldspar, opal-CT, quartz and dolomite are the main minerals in the fine-grained rocks associated with the trona beds. The trona crystals are generally white, massively bedded and exhibit a clear columnar crystalline texture, but locally they are grayish due to the presence of impurities. Trona formed as massive material and as separate crystals in the claystones and shales. In associated rocks, scattered euhedral trona crystals and crystal aggregates are present. Chemical analyses of trona and nahcolite ore samples are given in Table 4. Dolomite has been deemed the second most predominant mineral in the trona core samples. In the transition zone between the Çoraklar and Hırka formations, epsomite, hexahydrate, and starkeyite are abundant. In the uppermost rock unit of the Miocene sequence, sulfates become abundant (predominantly gypsum), bloedite is less abundant, and generally scarce thenardite and glauberite locally form thick sulfate deposits.

Petrographic studies indicate that several textures and fabrics are present in the trona beds. The dominant trona lithofacies developed at the sediment-brine interface and/or interstitially precipitated within upper part of the soft sediments. In this stage, trona crystals developed either as prismatic acicular crystals with palisade fabric or in radiating fans (Gündoğan and Helvacı, 2005). Pirssonite and rosette-like nodular-acicular trona minerals precipitated interstitially, mainly within the bituminous shale layers. Some of the crystalline, massive, matrix-free trona, and pure nahcolite beds seem to be direct precipitates from brine (Gündoğan and Helvacı, 2005). During the perennial alkaline-lake stage, bituminous shale accumulated first and, subsequently, some of zeolite minerals (mainly analcime) developed authigenically within those sediments. When the lake level dropped due to evaporation, pirssonite precipitated as the primary saline mineral. Two types of pirssonite crystallization are recognized: the first mainly developed displacively as euhedral crystals within bituminous shale; the second occurs as laminated varve-like alternations with bituminous shale. Pirssonite partially replaces analcime. During extensive evaporation, the Na/Ca ratio increased with declining lake-water level, and the rosette-like nodular-acicular

TABLE 3. CARBONATES AND OTHER MINERALS OCCURRING IN THE BEYPAZARI TRONA DEPOSIT OF THE HIRKA FORMATION

<u>SULFIDES</u>		<u>SILICATES</u>	
<b>Pyrite</b>	FeS <sub>2</sub>	Clay minerals	Smectite (Saponite) Illite Chlorite Montmorillonite
<u>OXIDES</u>		Loughlinite	Na <sub>2</sub> Mg <sub>3</sub> Si <sub>6</sub> O <sub>16</sub> ·8H <sub>2</sub> O
Quartz	SiO <sub>2</sub>	Searlesite	NaBSi <sub>2</sub> O <sub>6</sub> ·H <sub>2</sub> O
<b>α - Quartz</b>	SiO <sub>2</sub>	Hornblende	NaKCaMgFeAl, SiAlO(OH)
<b>Opal-C.T.</b>		Tourmaline	NaMg <sub>3</sub> Al <sub>6</sub> B <sub>3</sub> Si <sub>6</sub> O <sub>27</sub> (OH) <sub>4</sub>
Hematite	Fe <sub>2</sub> O <sub>3</sub>	Epidote	Ca <sub>2</sub> (Al,Fe) <sub>3</sub> Si <sub>3</sub> O <sub>12</sub> (OH)
<u>CARBONATES</u>		Biotite	K(Fe,Mg) <sub>2</sub> AlSi <sub>4</sub> O <sub>10</sub> (OH) <sub>2</sub>
Nahcolite	NaHCO <sub>3</sub>	Muscovite	KAl <sub>2</sub> Si <sub>3</sub> AlO <sub>10</sub> (OH) <sub>2</sub>
<b>Trona</b>	Na <sub>2</sub> CO <sub>3</sub> ·NaHCO <sub>3</sub>	Lepidolite	K(Li,Al) <sub>3</sub> (Al,Si) <sub>4</sub> O <sub>10</sub> (OH,F) <sub>2</sub>
Termonatrite	Na <sub>2</sub> CO <sub>3</sub> ·2H <sub>2</sub> O	Phlogopite	KMg <sub>3</sub> (Si <sub>2</sub> AlO <sub>10</sub> )F <sub>2</sub>
Pirssonite	Na <sub>2</sub> CO <sub>3</sub> ·CaCO <sub>3</sub> ·2H <sub>2</sub> O	<b>Orthoclase</b>	KAlSi <sub>3</sub> O <sub>8</sub>
Brugnatelite	Mg <sub>9</sub> FeCO <sub>3</sub> (OH) <sub>13</sub> ·4 H <sub>2</sub> O	Microcline	KAlSi <sub>3</sub> O <sub>8</sub>
<b>Calcite</b>	CaCO <sub>3</sub>	High-sanidine	KAlSi <sub>3</sub> O <sub>8</sub>
<b>Dolomite</b>	CaCO <sub>3</sub> ·MgCO <sub>3</sub>	<b>Albite</b>	NaAlSi <sub>3</sub> O <sub>8</sub>
Magnesite	MgCO <sub>3</sub>	Natrolite	NaAl(SiO <sub>3</sub> ) <sub>2</sub> ·2H <sub>2</sub> O
Natron	Na <sub>2</sub> CO <sub>3</sub> ·10 H <sub>2</sub> O	Heaulandite	Na <sub>2</sub> Al <sub>2</sub> Si <sub>5</sub> O <sub>10</sub> ·2H <sub>2</sub> O
Gaylussite	Na <sub>2</sub> CO <sub>3</sub> ·CaCO <sub>3</sub> ·5H <sub>2</sub> O	Clinoptiolite	CaAl <sub>2</sub> Si <sub>7</sub> O <sub>18</sub> ·6H <sub>2</sub> O
<u>SULFATES</u>		Sanidine	NaCaKMgAlOSi <sub>7</sub> ·7H <sub>2</sub> O
Gypsum	CaSO <sub>4</sub> ·2H <sub>2</sub> O	Chabazite	KAlSi <sub>3</sub> O <sub>8</sub>
Hexahydrate	MgSO <sub>4</sub> ·6H <sub>2</sub> O	Mordenite	CaAl <sub>2</sub> Si <sub>4</sub> O <sub>12</sub>
Epsomite	MgSO <sub>4</sub> ·7H <sub>2</sub> O	Ferrierite	(Ca, Na <sub>2</sub> , K <sub>2</sub> ) Al <sub>2</sub> Si <sub>10</sub> O <sub>24</sub> ·5H <sub>2</sub> O
Bloedite	MgSO <sub>4</sub> ·Na <sub>2</sub> SO <sub>4</sub> ·4H <sub>2</sub> O	Heulandite	(Na, K) <sub>2</sub> Mg(Si, Al) <sub>10</sub> O <sub>24</sub> ·7H <sub>2</sub> O
<u>PHOSPHATES</u>			CaAl <sub>2</sub> Si <sub>7</sub> O <sub>18</sub> ·6H <sub>2</sub> O
		Apatite	Ca <sub>5</sub> (PO <sub>4</sub> ) <sub>3</sub> (OH,F,Cl)
		Collaphone	Ca <sub>5</sub> (PO <sub>4</sub> ) <sub>3</sub> CO <sub>3</sub> ·H <sub>2</sub> O

Note: The predominant minerals are in boldface.

TABLE 4. CHEMICAL ANALYSES (IN WT%) OF 16 TRONA AND THREE NAHCOLITE SAMPLES COLLECTED FROM DRILL HOLES IN THE BEYPAZARI TRONA DEPOSIT

Trona Samples																
Oxide (%)	SJ6-13	SJ6-16	SJ6-18	SJ6-23	SJ6-26	SJ6-28	SJ6-35	SJ6-40	SJ17A-6	SJ17A-8	SJ17A-9	SJ31-5	SJ31-16	SJ32-8	SJ9-17	
SiO <sub>2</sub>	0.11	0.43	0.66	0.26	0.53	1.65	1.92	1.04	2.43	1.64	0.70	1.25	1.49	0.39	0.79	
Al <sub>2</sub> O <sub>3</sub>	0.09	0.00	0.06	0.00	0.02	0.40	1.13	0.06	0.28	0.09	0.09	0.06	0.73	0.04	0.13	
*Fe <sub>2</sub> O <sub>3</sub> <sup>T</sup>	0.01	0.00	0.02	0.04	0.20	0.23	0.07	0.23	0.28	0.09	0.04	0.01	0.12	0.02	0.02	
MgO	0.35	0.46	0.54	0.57	0.41	2.08	1.15	1.08	1.70	1.00	0.73	0.37	1.29	0.32	0.76	
CaO	0.00	0.15	0.04	0.11	0.08	1.21	0.29	0.60	0.70	0.36	0.36	0.01	0.17	0.00	0.24	
Na <sub>2</sub> O	40.51	41.78	40.08	40.24	39.74	37.21	39.51	39.54	38.37	39.32	39.03	39.83	39.15	40.03	39.57	
K <sub>2</sub> O	0.01	0.01	0.02	0.03	0.04	0.12	0.06	0.06	0.17	0.06	0.02	0.03	0.43	0.01	0.04	
SO <sub>3</sub>	0.42	0.15	0.61	0.30	0.24	0.57	0.57	0.32	0.08	0.13	0.35	0.52	0.52	0.79	0.12	
CO <sub>2</sub>	28.39	29.67	28.46	29.28	28.22	29.63	28.05	28.07	27.25	27.92	29.01	28.28	29.26	28.25	28.98	
H <sub>2</sub> O	29.62	27.50	29.11	29.04	29.37	26.87	28.34	28.54	28.04	28.78	28.80	29.06	27.51	29.30	28.88	
TOTAL	99.51	100.51	99.60	99.87	98.85	100.07	99.54	99.54	99.30	99.39	99.13	99.42	100.67	99.15	99.53	
Nahcolite Samples																
Oxide (%)	S22-14	S35-13	S35-15													
SiO <sub>2</sub>	3.91	5.53	2.08													
Al <sub>2</sub> O <sub>3</sub>	0.77	0.61	0.03													
*Fe <sub>2</sub> O <sub>3</sub> <sup>T</sup>	0.32	0.32	0.12													
MgO	2.85	2.48	1.18													
CaO	1.55	3.96	0.20													
Na <sub>2</sub> O	33.18	29.73	35.76													
K <sub>2</sub> O	0.16	0.33	0.08													
SO <sub>3</sub>	0.30	0.08	0.19													
CO <sub>2</sub>	24.01	27.00	25.53													
H <sub>2</sub> O	32.23	29.83	35.07													
TOTAL	99.28	99.87	100.24													

\*Fe<sub>2</sub>O<sub>3</sub><sup>T</sup> : Fe<sub>2</sub>O<sub>3</sub> + 1.111 x FeO

TABLE 5. METAL OXIDE CONCENTRATIONS IN SOLID CORE SAMPLES FROM THE BEYPAZARI TRONA DEPOSIT, TURKEY

Sample I.D	Depth of sample (m)	As (ppm)	CaO (wt%)	Fe <sub>2</sub> O <sub>3</sub> (wt%)	K <sub>2</sub> O (ppm)	MgO (ppm)	Na <sub>2</sub> O (wt%)
SJ6-19	333.50	1	1.30	0.087	290	2.60	37.1
SJ6-27	355.00	1	0.78	0.046	220	0.74	41.2
SJ6-32	379.50	1	0.24	0.018	92	0.34	44.6
SJ6-33	383.00	1	0.38	0.015	52	0.56	45.3
SJ7-5	284.75	1	0.33	0.020	68	0.43	45.8
SJ9-19	366.70	1	0.02	0.007	63	0.21	46.0
SJ17A-6	398.50	2	0.50	0.056	210	0.94	42.3
SJ17A-10	425.00	2	0.07	0.006	73	0.09	46.9
SJ22-11	371.00	2	0.14	0.016	87	0.18	47.3
SJ22-13	380.00	2	0.26	0.029	170	0.53	54.7
SJ31-13	305.50	1	0.56	0.019	170	0.54	40.9
SJ31-18	314.90	<1	0.04	0.003	50	0.04	41.4
SJ31-29	366.00	<1	0.32	0.021	140	0.55	40.6
SJ32-10	267.55	<1	0.06	0.009	88	0.10	43.3
SJ35-15	224.80	3	0.25	0.064	290	0.84	35.3

trona lithofacies precipitated interstitially. Nodular trona occurrences replace precursor pirssonite. During ephemeral stages, many cyclic alternations with green claystone and fan-like prismatic trona, developed. With increasing concentration of Mg/Ca in the brine, dolomite and high Mg-calcite were precipitated, and the previously existing trona lithofacies was replaced by those minerals. Finally, all of the lithofacies were replaced by authigenic pyrite (Helvacı, 1998; Gündoğan and Helvacı, 2005; Gündoğan and Helvacı, 2006).

Zeolitization, dolomitization, and chloritization are rather widespread in the rock units associated with the trona deposit; these processes probably operated shortly after deposition or during diagenesis. The mineral components of the associated fine-grained sedimentary rocks of the trona beds consist of, in decreasing order, clay minerals, dolomite, calcite, analcime, K-feldspar, plagioclase, quartz, opal-CT and  $\alpha$ -quartz. The bituminous shales that enclose the upper and lower trona horizons are composed of analcime, dolomite, calcite, opal-CT, quartz, K-feldspar, and plagioclase (Table 3) (Fig. 8). Dolomite and K-feldspar are abundant in all lithological units of the Hirka Formation.

In the carbonate fractions of rock associated with the trona deposits, predominantly dolomite, in many cases calcite, as well as lesser magnesite and colophonite occur. However, in the tuff fractions, predominantly zeolites (analcime, wairakite, natrolite, and clinoptilolite) are present. K-feldspar (high-sanidine, microcline, and adularia), plagioclase (albite and anorthite), quartz, clays, muscovite, biotite and amphibole (mainly hornblende), and trace amounts of lepidolite, searlesite, apatite, tourmaline, and epidote are found (Table 3).

Montmorillonite, illite, saponite, and chlorite are the only clay minerals identified within in all of the samples studied, and occur as Mg-montmorillonite, Ca-montmorillonite, and K-montmorillonite. Illite is only a minor component and is distributed irregularly. Chlorite has a continuous distribution within the deposits and is relatively abundant near or within the tuff horizon (Table 3).

Helvacı et al., (1988) concluded that the clay minerals display a vertical zonation, for example:

illite (dominant) + moderately crystallized smectite  $\rightarrow$  well-crystallized smectite (dominant) + illite  $\rightarrow$  illite (dominant) + illite

This is indicative of changing geochemical conditions in the lake (with more-dilute or more-concentrated brine) environment, Smectite, as well as other authigenic minerals, formed by weathering of volcanic glass in an alkaline-lacustrine environment.

### Chemistry

The Beypazari trona deposit has abundant trona and dolomite, minor amounts of nahcolite, and trace amounts of S, Cl, Sr, As, and B. Variations in the chemistry of trona and nahcolite from Beypazari are interpreted to reflect the different phases of concentration that occurred in the perennial saline lakes. The

Beypazari deposit contains high-grade trona and nahcolite ores; their chemical compositions are given in Tables 4–7. In the deposit, the Na<sub>2</sub>O contents of the trona range between 37% and 41%, and those of the nahcolite between 29% and 36%. The soda minerals in the Beypazari deposit have minor amounts of impurities and trace elements and are high-grade ores, reaching up to 99% in some beds.

Mg and Si are present in the evaporitic and diagenetic minerals (e.g., Mg in dolomites) and in the claystone, mudstone, bituminous shale and tuff fractions, but mainly in the latter. Al and Fe oxides are only present in the clays, bituminous shales, and tuffs (e.g., Fe in pyrites). During diagenesis, chemical exchange between evaporites, clays, tuffs, and bituminous shales occurred and led to the formation of diagenetic and authigenic minerals, such as pyrite, dolomite, K-feldspar, and analcime.

The Na-carbonate minerals were chemically precipitated from brines; these brines may have been partly derived from thermal springs and partly from surface streams and underground waters. Major-element compositions of the nearby volcanic rocks and granites are given in Tables 1 and 2; all of the rocks are enriched in Na relative to the average values for these rock types. Some clay minerals in the trona deposit have been derived from weathering of the tuff. Surface streams and underground waters may have carried dissolved Na, Mg, HCO<sub>3</sub>, and CO<sub>3</sub> into the basins from weathering of rocks exposed in the catchment area, but the major source of dissolved ions in the perennial saline lake is thought to have been from leaching of the Neogene volcanic rocks by thermal springs associated with volcanic activity in the area and by surface streams and underground waters.

In the system Na<sub>2</sub>O-H<sub>2</sub>O-CO<sub>2</sub>—the main composition of some saline lakes—the activity of water was the most important factor affecting the stability limits of the mineral phases. In addition, the partial pressure of CO<sub>2</sub> ( $P_{CO_2}$ ) is also one of the descriptive variables of the system. In ancient and present-day lakes, nahcolite, trona, natron, thermonatrite, wegscheiderite (Na<sub>2</sub>CO<sub>3</sub>·7H<sub>2</sub>O) and Na<sub>2</sub>CO<sub>3</sub>·10H<sub>2</sub>O, may be present as mineral phases; the Na<sup>+</sup> activity, pH and  $P_{CO_2}$  of the deposits are useful in determining the chemical conditions of some ancient lakes.

The middle Miocene atmosphere had a higher partial pressure of CO<sub>2</sub> than the present-day atmosphere (e.g., Warren, 2010). During deposition of the upper trona horizon, however, the partial pressure of CO<sub>2</sub> had decreased (relative to that of the lower trona horizon) in so far as nahcolite is not present in the lower trona beds.

### DEPOSITIONAL ENVIRONMENT OF THE HIRKA FORMATION AND THE TRONA DEPOSIT

The Beypazari Miocene sequence comprises coarse- to fine-grained sedimentary rocks with trona, lignite and bituminous shale deposits, carbonates and volcanic rocks. Based upon the lithological features of these rock units, it is concluded that the rocks were deposited within fluvial, lacustrine, and playa-lake environments. Laterally, the lacustrine and playa-lake

TABLE 6. CONCENTRATION OF AREAS AND IMPURITIES (FROM TITRATION) IN SELECTED BEYPAZARI TRONA AND NAHCOLITE SAMPLES, BEYPAZARI BASIN, TURKEY

Sample I.D.	Depth of sample (m)	Trona (wt%)	Nahcolite (wt%)	Insols (wt%)	NaCl (wt%)	Total (wt%)	Na <sub>2</sub> SO <sub>4</sub> (ppm)	Ba (ppm)	B (ppm)	Li (ppm)	P (ppm)	Sr (ppm)	Mn (ppm)	Ti (ppm)
SJ6-19	333.50	86.0		11.7	0.07	97.8	<25	21	436	46	35	78	45	55
SJ6-27	355.00	93.0		5.6	0.04	98.6	<25	17	816	34	37	42	10	28
SJ6-32	379.50	98.0		1.1	0.03	99.1	<25	<10	379	13	<10	<10	19	<10
SJ6-33	383.00	97.3		1.4	0.03	98.7	<25	13	339	14	171	27	<10	10
SJ7-5	284.75	98.0		1.0	0.03	99.0	<25	<10	315	15	124	22	14	<10
SJ9-19	366.70	98.7		0.2	0.03	98.9	<25	<10	301	21	11	<10	<10	<10
SJ17A-6	398.50	95.8		3.3	0.04	99.1	<25	<10	296	37	29	29	13	33
SJ17A-10	425.00	99.3		0.1	0.03	99.4	<25	<10	274	15	46	<10	<10	<10
SJ22-11	371.00	99.2		0.4	0.03	99.6	<25	<10	239	16	65	<10	<10	<10
SJ22-13	380.00	95.9		2.7	0.03	98.6	<25	12	256	31	22	18	<10	19
SJ31-13	305.50	95.9		3.0	0.03	98.9	<25	<10	231	20	26	30	21	<10
SJ31-18	314.90	100.0		0.1	0.03	100.1	<25	<10	212	10	18	<10	<10	<10
SJ31-29	366.00	97.1		2.0	0.03	99.1	<25	<10	239	28	20	11	<10	20
SJ32-10	267.55	99.3		0.0	0.03	99.4	<25	<10	197	14	14	<10	<10	<10
SJ35-15	224.80	14.6	78.2	4.4	0.03	97.2	<25	<10	157	42	42	14	<10	31

TABLE 7. ANALYSES OF TRONA ORE CONCENTRATIONS AND IMPURITIES IN SAMPLES FROM TRONA BEDS 11 AND 15 IN DIFFERENT DRILL HOLES, BEYPAZARI TRONA DEPOSIT

Drill hole	Surface elevation	Trona bed	Top depth	Bottom depth	Thickness	% Trona	% Other
SJ-32	998.66	11	261.20	265.06	4.40	93.66	6.34
SJ-10	890.84	11	344.15	348.95	4.80	94.00	6.00
		15	319.40	323.15	3.75	93.49	6.51
SJ-17A	854.71	11	425.10	427.90	2.80	94.27	5.73
		15	397.95	402.85	4.90	86.03	13.97
SJ-6	847.92	11	342.85	348.30	5.45	95.45	4.55
		15	320.75	325.55	4.80	94.73	5.27
SJ-9	868.67	11	304.65	304.65	5.30	87.75	12.25
		15	285.65	285.65	2.75	60.53	39.47

Note: Surface elevations in meters above mean sea level; depths in meters below surface.

environment sediments intertongue with fluvial sediments, and the Bey pazari basin represent a restricted, evaporite-rich cycle of deposition (Fig. 13).

The Hirka Formation comprises dolomitic claystone, bituminous shale, trona, and intraformational conglomerate lithofacies, all deposited in a lacustrine depositional system (Fig. 5).

**Dolomitic-Claystone Lithofacies**

This lithofacies consists mainly of light green, thick-bedded, partially laminated claystone and minor amounts of mudstone (Fig. 5). The dolomite is present as euhedral authigenic crystals and microcrystalline matrix in the claystone and mudstone. In these fine-grained rocks, dolomite is the second most abundant mineral constituent (Helvacı et al., 1988). Framboidal pyrite grains are abundant in the claystone beds. Thin, analcitized tuff and green siltstone layers are minor lithologies within this lithofacies.

**Bituminous-Shale Lithofacies**

The bituminous-shale lithofacies comprises two main rock types: thinly laminated, organic-matter-rich, dark-gray and brown bituminous shale, and brecciated bituminous shale. Brecciated bituminous shale has been observed in drill-cores acquired during trona exploration (Fig. 5). A similar rock type has also been noted by Bradley (1931), and Eugster and Hardie (1975) in the Green River and Bridger formations of the Piceance Creek and the Uinta basins.

The rocks associated with the bituminous-shale lithofacies are thin dolomitic limestone, shale, and tuff interlayers. The results of chemical analyses of tuffs are given in Table 8.

**Intraformational–Conglomerate Lithofacies**

This lithofacies is represented by intraclastic conglomerate composed of tuff, limestone, bituminous shale and dolomite clasts derived from the underlying or adjacent rock units. The conglomerate exhibits six different layers, ranging from ~80 cm to 10 m in thickness, in the coal-mine tunnel section near the town of Çayırhan (Fig. 5, section G-2001). Large- and small-scale slumps, slides and fining-upward grading are widespread structures. The lower contact of the conglomerate beds is generally erosional, and the upper contact is gradational into green claystone, which contains small bituminous shale clasts (Fig. 5).

The intraformational conglomerate also deposited alternately with trona in the northeastern part of the basin. The dominant clasts of the conglomerate are tuff and limestone, minor amounts of trona, dolomite and bituminous shale of ~2 cm in size, and they are supported by a tuffaceous matrix.

**Environmental and Depositional Interpretation of the Trona Deposit and Associated Rock Types**

The bituminous shale, trona, dolomitic claystone, and intraformational-conglomerate lithofacies of the Hirka Formation covers an area of ~500 km<sup>2</sup> in the Bey pazari Miocene basin. The

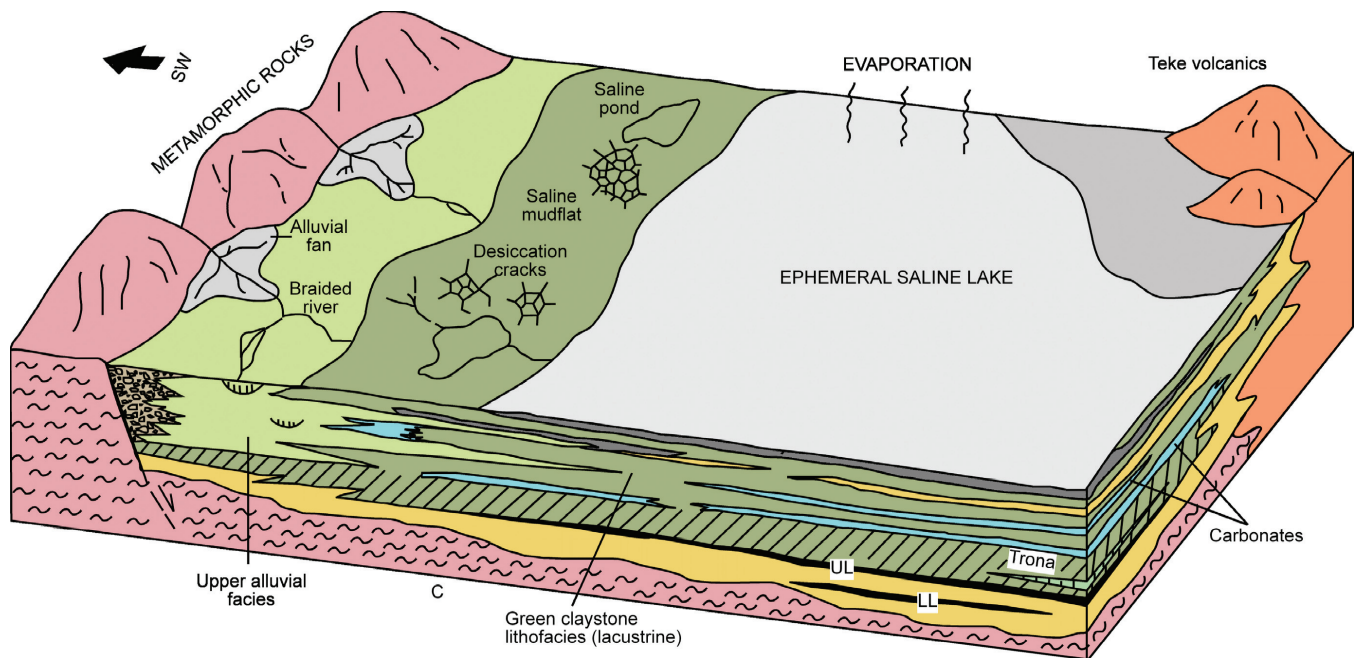


Figure 13. Schematic block diagram showing the depositional environments throughout the Miocene in the Bey pazari basin (not to scale).

TABLE 8. MAJOR OXIDE COMPOSITION (IN WT%) OF TUFF SAMPLES FROM THE HIRKA FORMATION, BEYPAZARI BASIN

Oxide (%)	K2-5	K8-14	K8-15	K8-18	SJ17A-15	SJ32-15	SJ32-26
SiO <sub>2</sub>	71.96	59.02	60.05	74.66	52.98	38.16	59.00
Al <sub>2</sub> O <sub>3</sub>	15.62	5.20	17.27	10.83	10.51	10.05	12.53
*Fe <sub>2</sub> O <sub>3</sub> <sup>T</sup>	0.62	1.13	6.30	2.24	4.29	1.43	3.02
MgO	0.03	3.37	0.59	0.00	2.68	6.73	1.02
CaO	1.72	8.08	0.92	0.00	7.52	9.05	7.38
Na <sub>2</sub> O	3.02	0.24	1.07	0.10	2.82	7.88	1.58
K <sub>2</sub> O	2.11	2.50	7.8	8.56	5.00	1.47	2.39
TiO <sub>2</sub>	0.45	0.75	1.00	0.65	0.55	0.25	1.05
P <sub>2</sub> O <sub>5</sub>	0.00	0.00	0.15	0.00	0.11	0.00	0.12
MnO	0.06	0.04	0.06	0.00	0.04	0.03	0.09
SO <sub>3</sub>	0.60	0.57	0.83	0.77	0.53	0.55	0.53
CO <sub>2</sub>	0.47	9.87	0.64	0.00	5.38	5.78	4.88
H <sub>2</sub> O	3.36	8.96	2.75	2.05	6.68	18.09	5.74
TOTAL	100.02	99.73	99.43	99.86	99.09	99.47	99.33

\*Fe<sub>2</sub>O<sub>3</sub><sup>T</sup>: Fe<sub>2</sub>O<sub>3</sub> + 1.111 × FeO

thickest sequence of this association is present on the north side of the Davutoğlan fault near Zaviye village. An ephemeral salt lake or very small closed lake must be visualized as the trona-brine body (with a normally dry surface) in this area—that is, near the transitional zone of the Hirka Formation and Teke volcanics. The trona was deposited in this environment.

Solutions were contributed primarily by thermal and alkaline springs that originated from the alkaline Teke volcanics and pre-Miocene granitic rocks situated south of Beypazarı (Table 9).

The dolomitic claystones probably formed on a playa flat, as originally described for the mudstone facies of the Green River Formation (Eugster and Surdam, 1973; Eugster and Hardie, 1975; Hardie et al., 1978; Youxun, 1983). The playa flat in the Beypazarı basin covered the westernmost part of the basin. At some localities in the Hirka Formation near Çayırhan, fibrous magnesium-sulfate minerals—such as epsomite and starkeyite—

filled desiccation cracks in the claystones. These mudcrack infillings are generally covered by bituminous shales. The absence of gypsum and the abundance of framboidal pyrite in the Beypazarı area may be explained by bacterial sulfate reduction. These kinds of mineral enrichments can originate via the biochemical contributions of algae that contributed to the formation of bituminous shales, as explained in Desborough (1978), and that settled into the bituminous shale during postdepositional periods.

The intraformational-conglomerate lithofacies indicates six major periods of synsedimentary deformation and transformation during deposition of the lithofacies associations of the Hirka Formation (Fig. 5). These deformations were caused by the NE-SW-trending Davutoğlan fault. During deposition of the intraformational conglomerate, the rocks and semiconsolidated sediments of the mud flat and very shallow-lake environments were probably eroded by surface flushing and flow, and then

TABLE 9. CHEMICAL ANALYSES, IN PARTS PER MILLION, OF THERMAL SPRINGS, MINERAL WATER, AND ARTESIAN WATER FROM THE BEYPAZARI AREA

Elements	Sj-8 artesian water	Ayaş thermal well springs	Dutlu-Tahtalı thermal springs			Beypazarı-Karakoca mineral water
	1	2	3	4	5	6
Na	6055.60	4609.00	1336.00	1453.00	1624.00	154.00
K	56.00	57.00	32.00	36.00	12.00	16.00
Ca	1.00	471.40	445.80	493.70	182.40	171.50
Mg	1.00	135.90	106.50	121.70	36.20	209.50
Sr	0.50	10.86	9.15	9.97	2.55	1.02
Ba	0.19	0.04	0.04	0.03	0.02	0.05
As	0.50	0.05	0.05	0.05	0.05	0.05
B	386.25	10.63	5.05	5.73	5.48	0.42
Li	0.31	1.65	0.91	1.00	0.48	0.46
Cl	2300	2200.00	1100.00	—	1200.00	16.00
F	7.30	n.d.	n.d.	—	n.d.	n.d.
SO <sub>4</sub>	155.00	3050.00	2330.00	—	2360.00	115.00
CO <sub>3</sub>	10.00	<0.1	<0.1	—	<0.1	<0.1
HCO <sub>3</sub>	2500.00	810.00	480.00	—	200.00	1100.00
Na/Ca+Mg	3027.5	7.59	2.42	2.36	7.43	0.40

Note: n.d.—not determined; dashes—negligible value or undetected.



redeposited in the depocenter located in the northeastern part of the basin (Fig. 6 and 13).

The lithofacies units of the Hirka Formation are interpreted to have been deposited in a playa-lake-type environment similar to that described by Eugster and Surdam (1973). Playa-lake deposition has been discussed and corroborated for the Green River Formation by various workers (Bradley and Eugster, 1969; Bradley, 1973; Wolfbauer and Surdam, 1974; Eugster and Hardie, 1975; Surdam and Wolfbauer, 1975; Lundell and Surdam, 1975; Surdam and Stanley, 1979; Helvacı, 1998). The dolomitic claystone lithofacies were deposited in the lake-margin playa and/or mud flat. Thick trona beds were deposited in a small, periodically drying closed-lake which was situated in the eastern part of this playa flat. This lake was supplied by alkaline-rich surface streams and underground waters that originated from adjacent volcanic and granitic rocks and playa flats. The bituminous-shale lithofacies was deposited in a shallow, brackish-water lake environment which expanded with seasonal flooding. Characteristics of the intraformational-conglomerate lithofacies indicate intra-basinal erosion, redeposition, and sediment selection toward the depositional center of the trona deposit.

The Neogene basin is partly filled by the products of adjacent coeval volcanic activity, which are situated in the northeastern part of the study area. These volcanic rocks are the likely source of Na for the precipitation of the trona and other Na-carbonate salts. The most likely sources of Na for the formation of the trona deposit were alkaline surface and underground waters and thermal springs, the weathering of rocks in the source area (granites and Cretaceous-Paleocene volcanic rocks), leaching of the tuffs interbedded with the sediments, and the extensive Teke volcanics interfingering with sediments in the NE part of the Beypazari basin (Helvacı, 1998; Figs. 6 and 13).

#### APPENDIX: DESCRIPTIONS OF FIELD STOPS IN THE BEYPAZARI MIOCENE BASIN



Figure A1 (Stop 1). Kirmir Formation consisting claystones and gypsums of the Beypazari basin, near the Gömleksiz bridge, by the road just before the entrance of the Beypazari town.

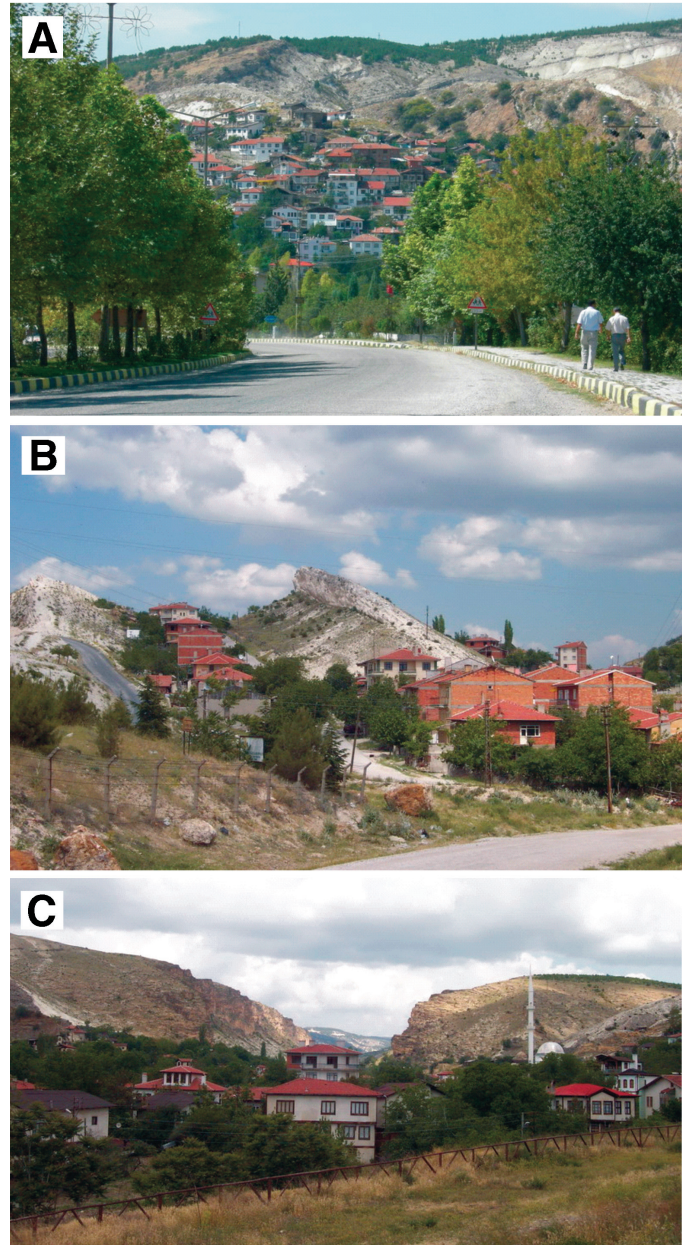


Figure A2 (Stop 2). (A) Main entrance to Beypazari town (part of Beypazari town with Miocene rocks cropping out in the background). (B) Flanks of the Beypazari flexure with houses located upon the flexure structure. (C) Overlooking İnozü valley from the entrance to Beypazari town; the İnozü tuff member of the Teke volcanics occurs in the background.



Figure A3 (Stop 3). The İnözü tuff member of the Teke volcanics overlying the shale and bituminous shale member of the Hırka Formation.



Figure A4 (Stop 4). Panoramic view of İnözü valley showing monoclinical folds that affected the Miocene Beypazarı basin. Here, the Teke volcanics (lavas) interfinger with the Hırka Formation as seen in the photograph.



Figure A6 (Stop 6). The Adaviran Basalt of the Teke volcanics occurs over a vast area in the northeastern part of the Beypazarı basin.



Figure A7 (Stop 7). (A) Outcrop of the Beypazarı granites and upper section of the Beypazarı Miocene sequence unconformably overlying them. Location Tahir, Oymağaç and Kırbaşı areas, SW of Beypazarı town. (B) Shown are xenoliths in the granite and typical holocrystalline texture of the granite.



Figure A5 (Stop 5). Close-up view of the interfingering of the Teke volcanics (lavas) with the Hırka Formation in the İnözü valley, northeastern part of the Beypazarı basin. Baking of the shales at the contact with lavas can be examined here.

**A**

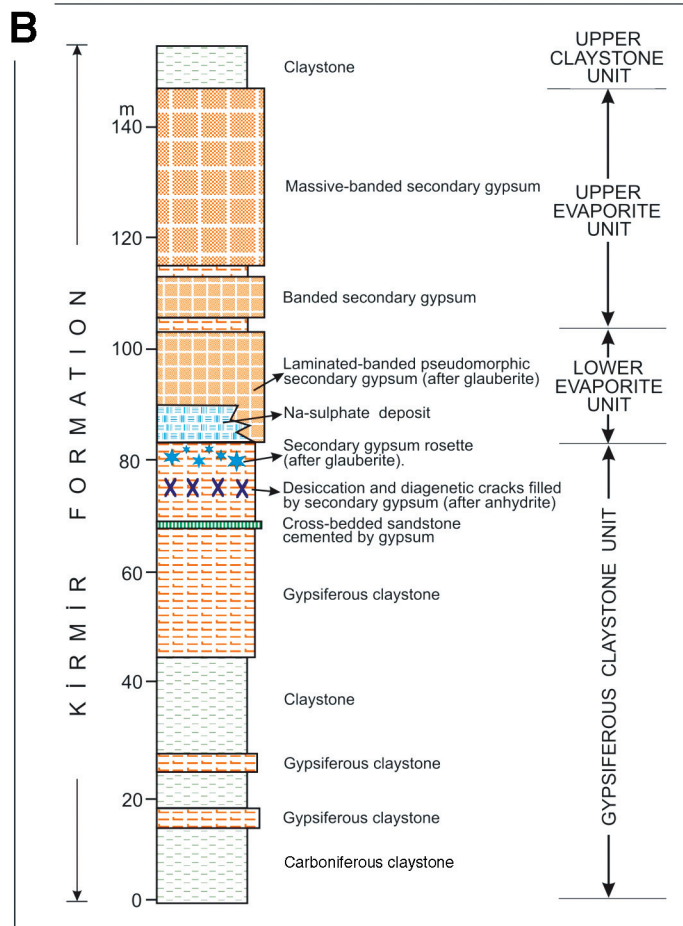


Figure A8 (Stop 8). (A–B) An outcrop photograph of the gypsiferous member of the Kirmir Formation. The facies are, from bottom to top: gypsiferous claystone facies with gypsum roses and mudcracks filled by gypsum; thenardite-glauberite facies; crystalline gypsum; laminar gypsum; and crystalline and massive gypsum facies. The vertical thickness of these strata is approximately 30 m. Location near Kirmir valley between the towns of Beypazarı and Çayırhan.



Figure A9 (Stop 9). Overview of Çayırhan town; a section of the Bozbelen and Kirmir formations as seen from the Çayırhan coal-mine residential area. From top to bottom: gypsum and gypsiferous claystone of the Kirmir Formation; Bozbelen Formation and Çayırhan Formation.



Figure A10 (Stop 10). Çayırhan dome structure, where the coal-bearing Çoraklar Formation, trona-bearing Hırka Formation and Akpınar Formation (at the top) are well exposed, with mutually gradational contacts (just NW of Çayırhan town).



Figure A11 (Stop 11). (A) Davutoğlan normal fault, trending NE-SW and displacing mainly the upper section of the Beypazarı Miocene sequence (NW of Çayırhan town). (B) At the same location in the foreground, the Çoraklar, Bozbelen, and Kirmir formations of the Beypazarı basin are well exposed. Lacustrine olive-green claystone lithofacies of the Çayırhan Formation. Red sandstone/mudstone fluvial deposits of the Bozbelen Formation and the gypsum member of the Kirmir Formation occur at the top of the sequence.



Figure A12 (Stop 12). Karaköy village, where the Beypazarı Miocene sequence (Çoraklar, Hırka and overlying formations) rests on Paleozoic metamorphic rocks.

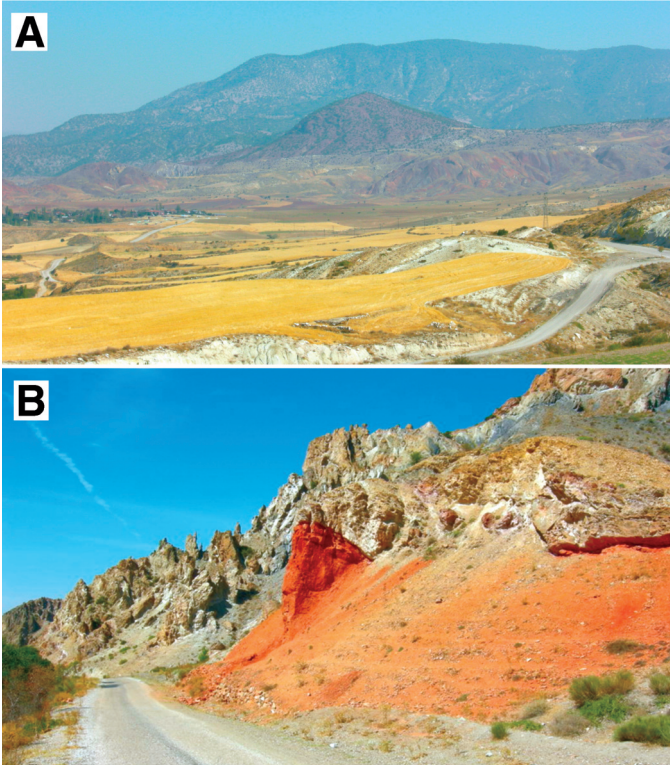


Figure A13 (Stop 13). (A) Photograph showing a part of the Nallıhan overthrust between Sekli and Hırka villages, where Paleozoic metamorphic rocks overthrust onto Paleocene red clastic rocks of the Kızılçay group around Hırka Village. Lower Tertiary clastic rocks; Paleozoic metamorphic rocks; and angular unconformity between Miocene rocks and basement rocks. (B) Overthrusting of the Paleozoic metamorphic rocks onto the Lower Tertiary rocks



Figure A14 (Stop 14). Here the Hırka formation conformably overlying the Çoraklar Formation at Hırka village. This is the place from which the Hırka Formation takes its name and where its type section is located Hırkatepe coal mine. In ascending order, from bottom to top: volcanoclastic debris-flow deposits; upper lignite seams; bituminous shale and dolomitic claystone lithofacies (Hırka Formation); and lacustrine silicified limestone and green claystone lithofacies (Akpınar Formation).

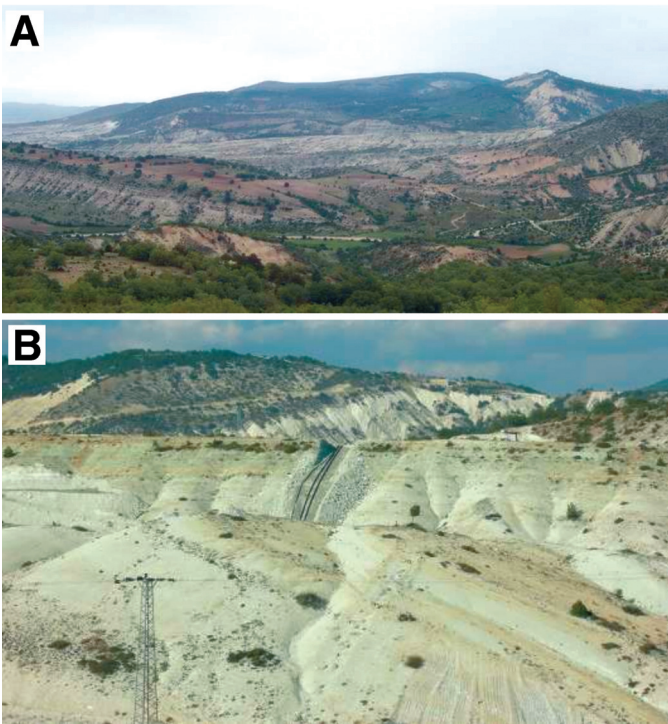


Figure A15 (Stop 15). (A–B) Trona field. Here, the Akpınar Formation overlies the Hurka Formation. Photograph also shows a flexure structure in the background. Trona beds are at depths between 350 and 450 m below the surface.

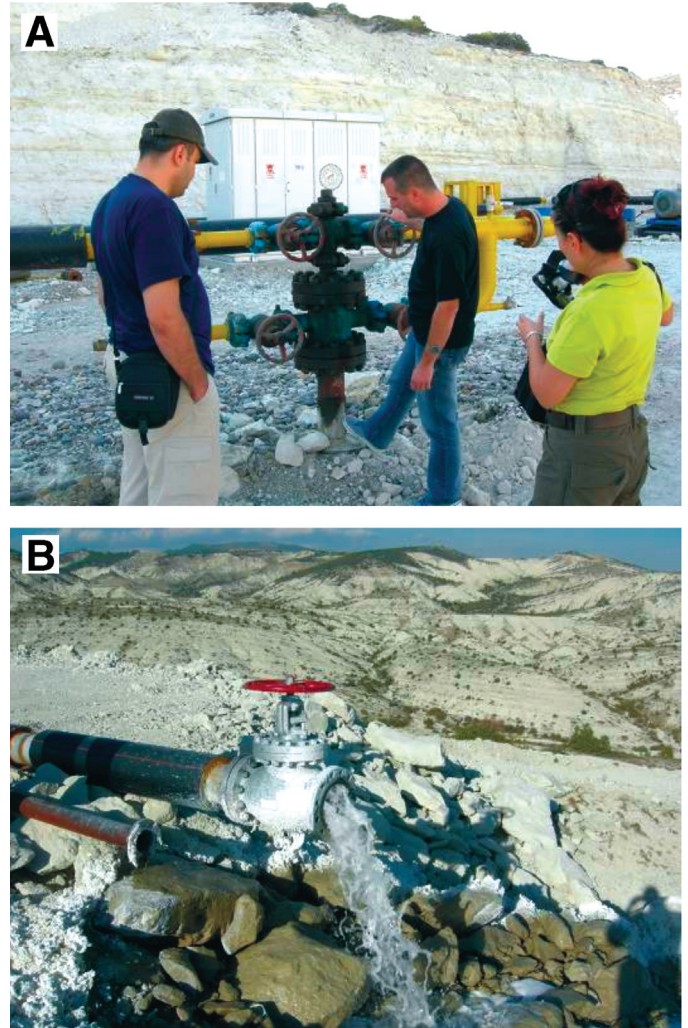


Figure A16 (Stop 16). (A) Pipelines for the trona-solution mines. (B) The solution exiting the pipe is sodium carbonate solution; near Zaviye village (NW of Beypazarı town).

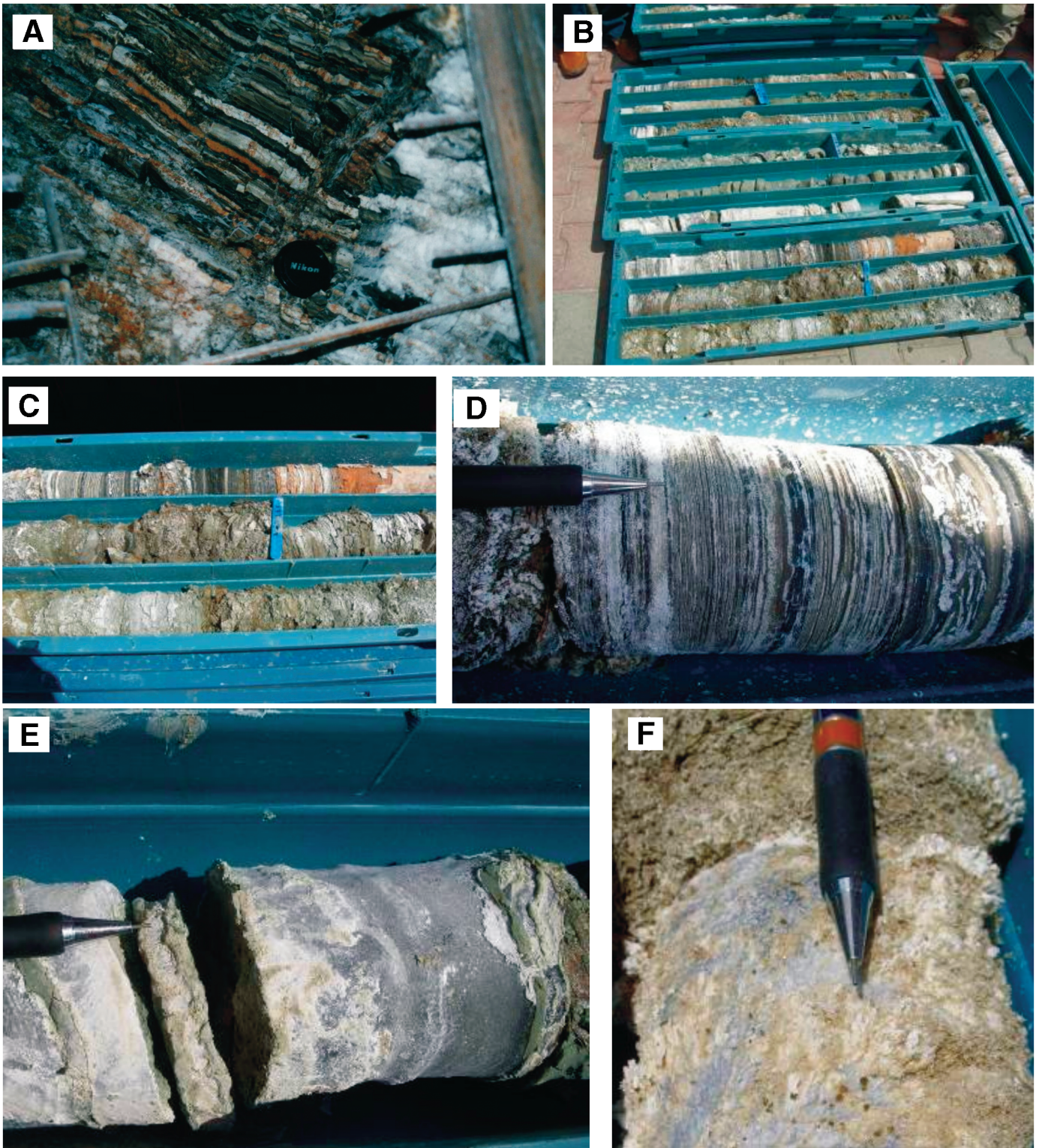


Figure A17 (Stop 17). (A) Interbedding of trona and bituminous shale beds in the main shaft of the trona mines. (B–D) Interbedding of trona and bituminous shale beds from drill holes. (E–F) Massive trona samples from drill holes.



Figure A18 (Stop 18). Beypazarı trona solvay process plant. Detailed information will be given by the staff of the plant.



Figure A19 (Stop 19). (A–B) Visit to the traditional Beypazarı bazaar and the old market and shopping area. After one-hour shopping break, return to Ankara.



## ACKNOWLEDGMENTS

Special thanks to Steve Mittwede for his specific comments and English editing of the text and to Yalçın Ersoy and Yeşim Yücel Öztürk for drafting assistance.

## REFERENCES CITED

- Altınlı, İ.E., 1973, Orta Sakarya'nın Jeolojisi: Cumhuriyetin 5. Yılı Yerbilimleri Kongresi, Ankara: Bulletin of the Mineral Research and Exploration Institute of Turkey, p. 159–191.
- Altınlı, İ.E., 1976, Geology of the northern portion of the Middle Sakarya River: İstanbul University, Fen. Fakültesi Mec: Section, v. 41, no. 1–4, p. 35–36.
- Altınlı, İ.E., 1977, Geology of the eastern territory of Nallıhan (Ankara province): İstanbul University, Fen Fakültesi Mec: Seri B. v. 42, no. 1–2, p. 29–44.
- Birön, C., Eskikaya, S., and Eskikaya, T., 1979, Türkiye Komur İşletmeleri Kurumu Beypazarı bitümlü sistlerin kazılabilirlik ve yanabilirlik etudu: Technical University, İstanbul, Report 4, 143 p.
- Bradley, W.H., and Eugster, H.P., 1969, Geochemistry and paleolimnology of the trona deposits and associated authigenic minerals of the Green River Formation of Wyoming: U.S. Geological Survey Professional Paper 496-B, 71 p.
- Bradley, W.H., 1931, Origin and microfossils of the oil shale of the Green River Formation of Colorado and Utah: U.S. Geological Survey Professional Paper 168, 58 p.
- Bradley, W.H., 1973, Oil shale formed in desert environment, Green River Formation, Wyoming: Geological Society of America Bulletin, v. 84, p. 1121–1123, doi:10.1130/0016-7606(1973)84<1121:OSFIDE>2.0.CO;2.
- Damon, P.E., Shafiqullah, M., and Clark, K.F., 1983, Geochronology of the porphyry copper deposits and related mineralization of Mexico: Canadian Journal of Earth Sciences, v. 20, p. 1052–1071.
- Desborough, G.A., 1978, A biogenic-chemical stratified lake model for the origin of oil shale of the Green River Formation: an alternative to the playa-lake model: Geological Society of America Bulletin, v. 89, p. 961–971, doi:10.1130/0016-7606(1978)89<961:ABSLMF>2.0.CO;2.
- Dündar, A., 1988, Ankara-Beypazarı trona deposit, geology and mineralogical characteristics: Industrial Minerals, (March, Supplement) p. 41–43.
- Eugster, H.P., and Hardie, L.A., 1975, Sedimentation in an ancient playa-lake complex: The Wilkins Peak Member of the Green River Formation of Wyoming: Geological Society of America Bulletin, v. 86, p. 319–334, doi:10.1130/0016-7606(1975)86<319:SIAAPC>2.0.CO;2.
- Eugster, H.P., and Surdam, R.C., 1973, Depositional environment of the Green River Formation of Wyoming: a preliminary report: Geological Society of America Bulletin, v. 84, p. 1115–1120, doi:10.1130/0016-7606(1973)84<1115:DEOTGR>2.0.CO;2.
- Gündoğan, İ., and Helvacı, C., 2001, Sedimentological and Petrographical Aspects of Upper Miocene Evaporites in the Beypazarı and Çankırı-Çorum Basins, Turkey: International Geology Review, v. 43, p. 818–829, doi:10.1080/00206810109465049.
- Gündoğan, İ., and Helvacı, C., 2005, Mineralogy, petrography and diagenetic aspects of the Beypazarı trona deposit, Middle Miocene, Turkey, ESCA 2005- İzmir, Abstracts, p. 44–45.
- Gündoğan, İ., and Helvacı, C., 2006, Beypazarı trona yatağında otijenik mineral oluşumları, 59: Türkiye Jeoloji Kurultayı, 20–24 Mart 2006, Ankara, Bildiri Özetleri Kitabı, p. 278–279.
- Hardie, L.A., Smoot, J.P., and Eugster, H.P., 1978, Saline lakes and their deposits: a sedimentological approach, in Matter, A. and Tucker, M.E., eds., Modern and Ancient Lake Sediments: International Association of Sedimentology Special Publication, v. 2, p. 7–41.
- Helvacı, C., and Bozkurt, S., 1994, Geology, mineralogy and petrogenesis of Beypazarı (Ankara) granite: Bulletin of the Geological Society of Turkey, v. 37, no. 2, p. 31–42.
- Helvacı, C., and İnci, U., 1989, Beypazarı trona yatağının jeolojisi, mineralojisi jeokimyası ve yörenin trona potansiyeli: Türkiye Bilimsel ve Teknik Araştırma Kurumu. Temel Bilimleri Araştırma Grubu. Proje No: TBAG-685, 159 p.
- Helvacı, C., 1998, The Beypazarı trona deposit, Ankara province, Turkey, in Dyni, J.R., and Jones, R.W., eds., Proceedings of the First International Soda Ash Conference () Volume II: Wyoming State Geological Survey Public Information Circular 40, Laramie, p. 67–103.
- Helvacı, C., 2001, Doğal soda yatakları ve ekonomik önemleri: Türkiye Jeoloji Bülteni, Cilt 44, sayı 3, Ahyan Erler Özel Sayısı, s. 49–58.
- Helvacı, C., İnci, U., Yılmaz, H., and Yağmurlu, F., 1989, Geology and Neogene trona deposit of the Beypazarı region, Turkey: Turkish Journal of Engineering and Environmental Sciences (Doğa-TÜBİTAK). v. 13, no.2, p. 245–256.
- Helvacı, C., Yılmaz, H., and İnci, U., 1988, Beypazarı (Ankara) yöresi Neojen tortullarının kil mineralleri ve bunların dikey ve yanal dağılımı: Jeoloji Mühendisliği, v. 32–33, p. 33–42.
- İnci, U., 1991, Miocene alluvial fan-alkaline playa lignite-trona bearing deposits from an inverted basin in Anatolia: sedimentology and tectonic controls on deposition: Sedimentary Geology, v. 71, p. 73–97, doi:10.1016/0037-0738(91)90008-2.
- İnci, U., Helvacı, C., and Yağmurlu, F., 1988, Stratigraphy of Beypazarı Neogene basin, Central Anatolia, Turkey: Newsletter for Stratigraphy, v. 18, no. 3, p. 165–182.
- Kalafatçıoğlu, A., and Uysallı, H., 1964, Geology of the Beypazarı-Nallıhan-Seben area: Bulletin of the Mineral Research and Exploration Institute of Turkey, v. 62, p. 1–12.
- Kayakıran, S., Akıncı, Ö., Çelik, E., and Dündar, A., 1986, Beypazarı trona yatağının jeolojisi: IVth Engineering Week, Isparta-Turkey, Abstracts, p. 75–76.
- Ketin, I., 1966, Tectonic units of Anatolia (Asia Minor): Bulletin of the Mineral Research and Exploration Institute of Turkey, v. 66, p. 23–34.
- Lundell, L.L., and Surdam, R.C., 1975, Playa-lake deposition, Green River Formation, Piceance Creek Basin, Colorado: Geology, v. 3, p. 493–497, doi:10.1130/0091-7613(1975)3<493:PDGRFP>2.0.CO;2.
- Narin, R., 1980, Beypazarı and Beyşehir lignite deposits in Central Anatolia, Turkey: Bulletin of the Geological Congress, Turkey, v. 2, p. 231–239.
- Nasün-Saygılı, G., Erdöl, N., Okutan, H., Yüzer, H., İşbilir, F., and Ekinci, E., 1974, Turkish trona, integrated process development and cost estimation: Industrial Minerals, April, p. 91–93.
- Önal, M., Helvacı, C., İnci, U., Yağmurlu, F., Meriç, E., and İzver, T., 1988, Stratigraphy, age, facies and depositional environments of the Soğukçam Limestone, Nardin Formation and Kızılçay Group in north of Çayırhan, northwest of Ankara: TAPG Bulletin, v. 1, no. 2, p. 152–163.
- Onargan, T., ve Helvacı, C., 2001, Ankara-Beypazarı doğal soda (trona) sahasının önemi ve işletme parametrelerinin irdelenmesi, 4: Endüstriyel Hammaddeler Sempozyumu, 18–19 Ekim 2001, İzmir, s. 155–162.
- Öngür, T., 1977, Kızılcahamam GB'sinin volkanolojisi ve petrografi incelemesi: TJK Bülteni, v. 20, p. 1–12.
- Orti, F., Gündoğan, İ., and Helvacı, C., 2002, Sodium sulphate deposits of Neogene age: the Kirmir Formation, Beypazarı Basin, Turkey: Sedimentary Geology, v. 146, p. 305–333.
- Saner, S., 1979, Explanation of the development of the Western Pontid Mountain and adjacent basins, based on plate-tectonic theory, northwestern Turkey: Bulletin of the Mineral Research and Exploration Institute of Turkey, v. 93, p. 1–20.
- Surdam, R.C., and Stanley, K.O., 1979, Lacustrine sedimentation during the culminating phase of Eocene Lake Gosiute, Wyoming (Green River Formation): Geological Society of America Bulletin, v. 90, p. 93–110, doi:10.1130/0016-7606(1979)90<93:LSDTCP>2.0.CO;2.
- Surdam, R.C., and Wolfbauer, C.A., 1975, Green River Formation, Wyoming: A playa-lake complex: Geological Society of America Bulletin, v. 86, p. 335–345, doi:10.1130/0016-7606(1975)86<335:GRFWAP>2.0.CO;2.
- Varol, B., and Kazancı, N., 1981, The litho- and biofacies properties of the Upper Jurassic-Lower Cretaceous carbonate sequence, in Nallıhan-Seben (Bolu) region: Bulletin of the Geological Society of Turkey, v. 24, p. 31–38.
- Warren, J.K., 2010, Evaporites through time: Tectonic, climatic and eustatic controls in marine and nonmarine deposits: Earth-Science Reviews, v. 98, p. 217–268, doi:10.1016/j.earscirev.2009.11.004.
- Wolfbauer, C.A., and Surdam, R.C., 1974, Origin of nonmarine dolomite in Eocene Lake Gosiute, Green River Basin, Wyoming: Geological Society of America Bulletin, v. 85, p. 1733–1740, doi:10.1130/0016-7606(1974)85<1733:OONDIE>2.0.CO;2.
- Yağmurlu, F., and Helvacı, C., 1994, Sedimentological characteristics and facies of the evaporite-bearing Kirmir Formation (Neogene), Beypazarı basin, Central Anatolia, Turkey: Sedimentology, v. 41, p. 847–860, doi:10.1111/j.1365-3091.1994.tb01428.x.
- Yağmurlu, F., Helvacı, C., İnci, U., and Önal, M., 1988, Tectonic characteristics and structural evolution of the Beypazarı-Nallıhan Neogene basin, Central Anatolia: METU Journal of Pure and Applied Sciences Series A: Geosciences, v. I, p. 127–143.
- Youxun, Z., 1983, Geology of the Wucheng trona deposit in Henan, China: Sixth International Symposium on Salt, The Salt Institute, v. 1, p. 67–73.